A NEW GENERATION CHEMICAL FLOODING SIMULATOR

Semi-annual Report for the Period
Sept. 1, 2001 – Feb. 28, 2002

By

Gary A. Pope, Kamy Sepehrnoori, and Mojdeh Delshad

Center for Petroleum and Geosystems Engineering

Work Performed under Contract No. DE–FC-26-00BC15314

Sue Mehlhoff, Project Manager

U.S. Dept of Energy

National Petroleum Technology Office

One West Third Street, Suite 1400

Tulsa, OK 74103-3159

Prepared by
The University of Texas
Center for Petroleum and Geosystems Engineering
Austin, TX 78712

A NEW GENERATION CHEMICAL FLOODING SIMULATOR

Contract No. DE–FC-26-00BC15314

The University of Texas
Austin, TX, 78712

Contract Date: October 1, 2001
Anticipated Completion: August 31, 2004
Government Award: $930,801 (Total funding)

Principal Investigators:
Gary A. Pope
Kamy Sepehrnoori
Mojdeh Delshad

Contract Officer:
Richard Rogus
National Petroleum Technology Office

Reporting Period: Sept. 1, 2001 – Feb. 28, 2002

ABSTRACT

The premise of this research is that a general-purpose reservoir simulator for several improved oil recovery processes can and should be developed so that high-resolution simulations of a variety of very large and difficult problems can be achieved using state-of-the-art computing and computers. Such a simulator is not currently available to the industry. The goal of this proposed research is to develop a new-generation chemical flooding simulator that is capable of efficiently and accurately simulating oil reservoirs with at least a million gridblocks in less than one day on massively parallel computers. Task 1 is the formulation and development of solution scheme, Task 2 is the implementation of the chemical module, and Task 3 is validation and application. We have made significant progress on all three tasks and we are on schedule on both technical and budget. In this report, we will detail our progress on Tasks 1 through 3 for the first six months of the project.

SUMMARY

During the past several years, an advanced and efficient reservoir simulation framework named IPARS, Integrated Parallel Accurate Reservoir Simulator (Parashar *et al.*, 1997) has been developed by the research team at the University of Texas. IPARS includes a number of advanced features such as providing all the necessary infrastructure for physical models, from message passing and input/output to solvers and well handling, run on a range of platforms, from a single PC with Linux Operating System to massively parallel machines or clusters of workstation. The framework supports isothermal, three-dimensional, multiple phases containing multiple species plus an immobile solid rock phase with adsorbing components. Phase densities and viscosities may be arbitrary functions of pressure and composition. Porosity and permeability may vary with location. Physical properties such as relative permeability and capillary pressure are functions of saturations and rock type. An arbitrary number of wells may be completed at arbitrary locations. Finite difference formulations with a block-centered grid are assumed in the framework. The nonlinear difference equations are solved by either fully implicit or semi-implicit techniques. Both mass balance and volume balance is supported. Since the portability of the simulator is very important, FORTRAN 77 is used

wherever possible. For memory management and user interaction, classical C is used. Commercial libraries are prohibited except in the graphics front end to the simulator. The simulator is formulated for a distributed memory, message passing machine. Free-format keyword input is used for direct data input. The simulator uses a single set of units to solve the partial differential equations. However, the user may choose any physically correct units for the input variables and they will then be converted to the default internal unit using appropriate conversion factor.

The overall structure of IPARS consists of 3 layers:

- Executive layer that consists of routines that direct the overall course of the simulation
- Work routines that are typically FORTRAN subroutines that perform grid element computations.
- Data-management layer that handles the distribution of grid across processing nodes, local storage allocation, dynamic reallocation and dynamic load balancing, and communication rescheduling. The data-management layer is also responsible for checkpoint/restart, input/output and visualization.

The fully implicit EOS compositional formulation has already been implemented into the IPARS framework and successfully tested. The Peng-Robinson EOS is used for hydrocarbon phase behavior calculations. The linear solvers from PETSc package are used for the solution of underlying linear equations. The framework provides hooks for implementing specific physical models. Such hooks bridge the models with the framework. There are several executive routines, and any communications between the processors and compositional model are performed in these routines. Many tests have been performed using the EOS compositional simulator on variety of computer platforms such as IBM SP and a cluster of PCs (Wang *et al.*, 1999).

The goal of this project is to add a chemical module to the existing compositional Peng-Robinson cubic equation of state (EOS). The simulator called GPAS, General Purpose Adaptive Reservoir Simulator, will then include the IPARS framework, and the

compositional and chemical modules as illustrated in **Figure 1.1**. In this report, we will detail our progress on Tasks 1 through 3 for the first six months of the project.

Task 1: Formulation and Development of Solution Scheme

The effort on this task was directed towards the formulation of tracer and polymer options. For completeness, we first give a brief review of the mathematical formulation of the compositional model. The assumptions made in developing the formulation are:

- Reservoir is isothermal.
- Darcy's law describes the multiphase flow of fluids through the porous media.
- Impermeable zones represented by the no-flow boundaries surround the reservoir.
- The injection and production of fluids are treated as source or sink terms.
- The rock is slightly compressible and immobile.
- Each hydrocarbon phase is composed of n_c hydrocarbon components, which may include the non-hydrocarbon components such as CO_2, N_2 or H_2S.
- Instantaneous local thermodynamic equilibrium between hydrocarbon phases.
- Negligible capillary pressure effects on hydrocarbon phase equilibrium.
- Water is slightly compressible and water viscosity is constant.

Mass conservation equation

The general mass conservation equation for species i in a volume V can be expressed as

{Rate of accumulation of i in V } **(1)**

= {Rate of i transported into V }

- {Rate of i transported from V }

+ {Rate of production of i in V }, $i = 1,\ldots, N_c$

The differential form for the species conservation equation can be expressed as:

$$\frac{\partial W_i}{\partial t} + \vec{\nabla} \bullet \overrightarrow{N_i} - R_i = 0 \qquad \textbf{(2)}$$

where W_i is the overall concentration of i in units of mass of i per unit bulk volume, $\overrightarrow{N_i}$ is the flux vector of species i in units of mass of i per surface area-time and R_i is the mass rate of production in units of mass of i per bulk volume-time.

The mass balance equation can be expressed in terms of moles per unit time by defining each term of Equation **(2** in terms of the porous media and fluid properties such as porosity, permeability, density, saturations, compositions, rates etc. The accumulation term for a porous medium becomes

$$W_i = \phi \sum_{j=1}^{n_p} \xi_j S_j x_{ij} \qquad \textbf{(3)}$$

where ϕ is the porosity, ξ_j is the molar density of phase j, S_j is the saturation of phase j and x_{ij} is the mole fraction of component i in phase j.

The flux vector of component i is a sum of the convective and the dispersive flux, and can be expressed as

$$\overrightarrow{N} = \sum_{j=1}^{n_p} \xi_j x_{ij} \overrightarrow{u_j} - \phi \xi_j S_j \overrightarrow{\overrightarrow{K_{ij}}} \bullet \vec{\nabla} x_{ij} \qquad \textbf{(4)}$$

where $\overrightarrow{u_j}$ represents the superficial velocity or flux of phase j. The flux is evaluated using the Darcy's law for multiphase flow of fluids through porous media.

$$\vec{u}_j = -\overrightarrow{\overrightarrow{K}} \lambda_{rj} (\vec{\nabla} P_j - \gamma_j \vec{\nabla} D) \qquad \textbf{(5)}$$

Darcy's law is a fundamental relationship describing the flow of fluids in permeable media under laminar flow conditions. The differential form of Darcy's law can be used to treat multiphase unsteady state flow, non-uniform permeability, non-uniform pressure gradients. It is used to govern the transport of phases from one cell to another under the local pressure gradient, rock permeability, relative permeability and viscosity. Converting each of the terms in the mass balance equation to units of moles per unit time and expressing the flux using Darcy's law, the mass balance for each component i is the following partial differential equation:

$$\frac{\partial}{\partial t}\left(\phi\sum_{j=1}^{n_p}\xi_j S_j x_{ij}\right)+\vec{\nabla}\bullet\left[\sum_{j=1}^{n_p}\xi_j\lambda_j x_{ij}(\vec{\nabla}P_j-\gamma_j\vec{\nabla}D)+\phi\xi_j S_j\overrightarrow{\overrightarrow{K_{ij}}}\bullet\vec{\nabla}x_{ij}\right]-\frac{q_i}{V_b}=0 \qquad \textbf{(6)}$$

Multiplying both sides of Equation **6** by V_b gives

$$V_b\frac{\partial}{\partial t}\left(\phi\sum_{j=1}^{n_p}\xi_j S_j x_{ij}\right)-V_b\vec{\nabla}\bullet\left[\sum_{j=1}^{n_p}\xi_j\lambda_j x_{ij}(\vec{\nabla}P_j-\gamma_j\vec{\nabla}D)+\phi\xi_j S_j\overrightarrow{\overrightarrow{K_{ij}}}\bullet\vec{\nabla}x_{ij}\right]-q_i=0 \qquad \textbf{(7)}$$

for $i=1,....,n_c$

The above equation is written is terms of moles per unit time, in which q_i is the molar injection (positive) or production (negative) rate for component i. The mobility for phase j is defined as

$$\lambda_j=\frac{kk_{rj}}{\mu_j} \qquad \textbf{(8)}$$

The physical dispersion term has not yet been implemented in GPAS.

Phase behavior and equilibrium calculations

The phase equilibrium relationship determines the number, amounts and compositions of all the equilibrium phases.

The sequence of phase equilibrium calculations is as follows:

1. The number of phases in a gridblock is determined using the phase stability analysis.
2. After the number of phases is determined, the composition of each equilibrium phase is determined.
3. The phases in the gridblock are tracked for the next time step calculations.

Phase Stability Analysis

The stability algorithm has not been implemented in EOSCOMP. One way of doing the phase stability analysis was given by Michelsen (1982). The Michelsen's approach could be used for the implementing the phase stability analysis in EOSCOMP as explained below.

A stability analysis on a mixture of overall hydrocarbon composition $\overline{Z}$ is a search for a trial phase, taken from the original mixture that, when combined with the remainder of the mixture, gives a value of Gibbs free energy that is lower than a single-phase mixture of overall hydrocarbon composition, $\overline{Z}$ (Michelsen, 1982 ; Trangenstein, 1987 ,Chang, 1990). If such a search is successful, an additional phase must be added to the phase equilibrium calculation. This condition is expressed mathematically as

$$\Delta G = \sum_{i=1}^{n_c} y_i \left[\mu_i(\overline{Y}) - \mu_i(\overline{Z}) \right] \qquad \textbf{(9)}$$

where μ_i is the chemical potential of component i and y_i is the mole fraction of component i in the trial phase. Thus, if for any set of mole fractions the value of ΔG at constant temperature and pressure is greater than zero, then the phase will be stable. If a composition can be found such that $\Delta G < 0$, the phase will be unstable.

The phase stability analysis is to solve the following set of nonlinear equations for the variables Y_i

$$\ln Y_i + \ln \phi_i(\overline{Y}) - h_i = 0 \qquad \textbf{(10)}$$

for $i = 1,.., n_c$

where the mole fraction $\overline{Y}$ and h_i is related to these variables by

$$y_i = \frac{Y_i}{\sum_{i=1}^{n_c} Y_s} \qquad \textbf{(11)}$$

$$h_i = \ln Z_i + \ln \phi_i(\overline{Z}) \qquad \textbf{(12)}$$

for $i = 1,....,n_c$

Flash calculation

Once a mixture has been shown to split into more than one phase by the stability calculation, the flash involves calculation of the mole fraction and composition of each phase at the given temperature, pressure and overall composition of the fluid. The

governing equations for the flash require equality of component fugacities and mass balance.

The equilibrium solution must satisfy three conditions:

- mass conservation of each component in the mixture
- chemical potentials for each component are equal in all phases
- Gibbs free energy at constant temperature and pressure is a minimum.

Fugacity is calculated using the Peng Robinson equation-of-state. The phase composition constraint, which says that the sum of the mole fraction of all the components in a phase equals to one, and the Rachford-Rice equation for determining the phase amounts for two hydrocarbon phases is implicitly used in the solution of the fugacity equation. The Rachford-Rice equation is used to determine the phase compositions and amounts. This equation requires the values of the equilibrium ratios K_i, which are defined as the ratio of the mole fractions of component i in oil and gas phases, respectively. The K_i values are determined by the equality of component fugacities in each phase. The fugacity equality, the Rachford-Rice equation and the Peng Robinson equation of state are described below in detail.

Equality of the Component Fugacity

One of the criteria for phase equilibrium is the equality of the partial molar Gibbs free energies or the chemical potentials. Alternatively, this criterion can be expressed in terms of fugacity (Sandler, 1999):

With the assumption of local thermodynamic equilibrium for the hydrocarbon phases, the criterion of phase equilibrium applies (Smith and Van Ness, 1975), namely

$$f_{ij} = f_{il} \quad \text{for } i = 1,.....n_c \qquad j = 2,.....n_p\,(j \neq l) \tag{13}$$

where phase l has been chosen as a reference phase. The fugacity of a component in a phase is taken as a function of pressure and phase composition, at a given temperature,

$$f_{ij} = f_{ij}\left(P, \overline{x_j}\right) \text{ for } i = 1,.....n_c \qquad j = 2,.....n_p\,(j \neq l) \tag{14}$$

Composition Constraint

The phase composition constraint is

$$\sum_{i=1}^{n_c} x_{ij} - 1 = 0 \tag{15}$$

where the mole fractions are defined as

$$x_{ij} = \frac{n_{ij}}{n_j} \tag{16}$$

for $i = 1,2,....n_c,\ j = 1,2,....,n_p$

Rachford-Rice Equation

In a classical flash calculation, the amount and composition of each equilibrium phase is evaluated using a material-balance equation after each update of the K-value from the equation-of-state:

$$r(v) = \sum_{i=1}^{n_c} \frac{(K_i - 1)Z_i}{1 + v(K_i - 1)} = 0 \tag{17}$$

where v is the mole fraction of gas in absence of water, K_i is the equilibrium ratio, Z_i is the overall mole fraction of component i in the feed and $r(v)$ is the residual of the Rachford-Rice equation.

The component mole fractions in the liquid and gas phases are then computed from the equations:

$$x_i = \frac{Z_i}{1 + v(K_i - 1)} \tag{18}$$

$$y_i = \frac{Z_i K_i}{1 + v(K_i - 1)} \tag{19}$$

The range for v is defined by

$$v_l = \frac{1}{1 - K_{\max}} < 0 \qquad \textbf{(20)}$$

$$v_r = \frac{1}{1 - K_{\min}} > 0$$

Equation **17** is a monotonically decreasing function of v with asymptotes at v_l and v_r. Usually, a Newton iteration can efficiently solve Equations **18** and **19** for v. However, round-off errors occur when solving Equation **17**.

Leibovici and Neoschil Equation

EOSCOMP solves the Rachford-Rice Equation. As was described above, round-off errors occur when solving the Rachford-Rice equation. To avoid the round off errors that occur when solving Equation **17**, the original Rachford-Rice equation can be changed into a form that is more nearly linear with respect to v as done by Leibovici and Neoschil (1992) and this approach could be implemented in EOSCOMP. The Leibovici and Neoschil equation is given by:

$$\tilde{r}(v) = (v - v_l)(v_r - v)\sum_{i=1}^{n_c} \frac{(K_i - 1)Z_i}{1 + v(K_i - 1)} = 0 \qquad \textbf{(21)}$$

The range for v is defined by

$$v_{\min} = \max\left(\frac{Z_i K_i - 1}{K_i - 1}\right) \qquad \textbf{(22)}$$

for $K_i > 1$ and $Z_i < 0$

$$v_{\max} = \min\left(\frac{Z_i - 1}{K_i - 1}\right) \qquad \textbf{(23)}$$

for $K_i < 1$ and $Z_i > 0$

Also, the Newton procedure is used to solve Equation **21** for v.

Equation of State

The Peng Robinson equation of state (Peng and Robinson, 1976) is

$$P = \frac{RT}{\underline{V} - b} - \frac{a(T)}{\underline{V}(\underline{V} + b) + b(\underline{V} - b)} \qquad \textbf{(24)}$$

The parameters a and b for a pure component are computed from

$$a(T) = 0.45724 \frac{R^2 T_c^2}{P_c} \alpha(T) \quad \textbf{(25)}$$

$$\sqrt{\alpha} = 1 + \kappa \left(1 - \sqrt{\frac{T}{T_c}} \right) \quad \textbf{(26)}$$

$$b = 0.07780 \frac{RT_c}{P_c} \quad \textbf{(27)}$$

$$\kappa = 0.37464 + 1.54226\omega - 0.26992\omega^2, \quad \textbf{(28)}$$

if $\omega < 0.49$

$$\kappa = 0.379640 + 1.485030\,\omega - 0.164423\,\omega^2 + 0.016666\,\omega^3 \quad \textbf{(29)}$$

if $\omega \geq 0.49$

For a multi component mixture, the mixing rules for the two parameters are

$$a = \sum_{i=1}^{N_c} \sum_{j=1}^{N_c} x_i x_j \sqrt{a_i a_j} (1 - k_{ij}) \quad \textbf{(30)}$$

and

$$b = \sum_{i=1}^{N_c} x_i b_i$$

where for component i, the a_i is computed from Equation **25**, and b_i is computed from Equation **27** The constant, k_{ij} is called the binary interaction coefficient between components i and j.

The Peng Robinson Equation of state can be written in the form

$$Z^3 + \alpha Z^2 + \beta Z + \gamma = 0 \quad \textbf{(31)}$$

where $Z = \frac{PV}{RT}$ is the compressibility factor, and the parameters are expressed as

$$\alpha = -1 + B \quad \textbf{(32)}$$

$$\beta = A - 3B^2 - 2B \quad \textbf{(33)}$$

$$\gamma = -AB + B^2 + B^3 \quad \textbf{(34)}$$

$$A = \frac{aP}{(RT)^2} \quad \textbf{(35)}$$

$$B = \frac{bP}{RT} \quad \textbf{(36)}$$

In GPAS, the equation-of-state calculations are done in the subroutine named XEOS, which contains the four subroutines EOSPURE, EOSMIX, EOSPHI and EOSPARTIAL. The equation-of-state parameters for each pure component are calculated in the subroutine EOSPURE. Mixture values are calculated in the subroutine EOSMIX. The fugacity coefficient is calculated from the equation-of-state in the subroutine EOSPHI and the equation-of-state related derivatives are computed in the EOSPARTIAL subroutine. The subroutine EOSCUB solves the Peng Robinson cubic equation-of-state and calculates the compressibility factor and its derivative. EOSCOMP requires the pure component critical temperature, critical pressure, critical volume, acentric factors, molecular weights and binary interaction coefficients to calculate the equation of state parameters. The volume shift parameter is not implemented in GPAS.

The main flash subroutine in GPAS is XFLASH. This subroutine performs the flash calculation at a given initial composition, temperature and pressure. The number of components, binary interaction coefficients and the equilibrium ratio values are also part of the input to this subroutine. An initial estimate of the equilibrium values is done in the subroutine STABL, which is then passed to the flash calculations. The flash subroutine calculates the liquid and vapor phase mole fractions, liquid and vapor compressibility factors, and also the negative residual of component i in cell k. The subroutine SOLVE solves the Rachford-Rice equation for finding the phase composition and the phase amounts.

Phase identification and tracking

Phase identification deals with the labeling of a phase as oil, gas, or aqueous phase at the initial conditions and also when a new phase appears. After a phase has been identified, phase tracking does the labeling of a phase during the simulation. Labeling phases consistently is important because of the need to assign a consistent relative permeability to each phase during a numerical simulation. Perschke (1988) developed a

method for the phase identification and tracking in which both phase mass density and phase composition are used. This is the procedure followed in GPAS. Once a phase has been identified, it is tracked during simulation by comparing the mole fraction value of a selected or key component in the equilibrium phases at the new time step with the values at the old time step. The phases at the new time step are labeled such that the mole fraction values are closest to the values at the old time step.

The algorithm used in GPAS for naming a phase when the hydrocarbon mixture is a single phase is similar to that proposed by Gosset et al. (1996). The parameters A and B of a two-parameter cubic EOS are computed from

$$A = \frac{aP}{(RT)^2} = \Omega_a \frac{PT_c^2}{P_c T^2} \alpha \qquad \textbf{(37)}$$

$$B = \frac{bP}{RT} = \Omega_b \frac{PT_c}{P_c T} \qquad \textbf{(38)}$$

where

$\Omega_a = 0.457235529$

$\Omega_b = 0.077796074$

Dividing Equation **37** by Equation **38** gives:

$$\frac{A}{B} = \frac{\Omega_a T_c}{\Omega_b T} \alpha \qquad \textbf{(39)}$$

where α is defined in Equation **26**.

A fluid is assumed to be in single-phase if $T > T_c$, which also implies $\alpha \leq 1$. From Equation **39**, this implies

$$\frac{A}{B} \leq \frac{\Omega_a}{\Omega_b} \qquad \textbf{(40)}$$

or its molar volume to be greater than the critical molar volume, $v > v_c$, which implies

$$Z > \frac{BZ_c}{\Omega_b} \qquad \textbf{(41)}$$

In GPAS, the subroutine EOS_1PH identifies a single phase as oil or gas using the above method. Also, an option is provided in the code to identify a single phase by

the conventional method: The fluid is liquid when sum of $Z_i K_i = 1$, and the fluid is gas when the sum of $Z_i / K_i = 1$.

Constraints and constitutive equations

Volume constraint

The volume constraint states that the pore volume in each of the cells must be filled completely by the total fluid volume. This is expressed in a mathematical form as

$$\sum_{i=1}^{n_c} N_i \sum_{j=1}^{n_p} L_j \overline{v_j} - V_p = 0 \qquad \textbf{(42)}$$

where N_i is the number of moles of each component i per unit bulk volume, L_j is the ratio of moles in phase j to the total number of moles in the mixture, $\overline{v_j}$ is the molar volume of phase j, and V_p is the pore volume of a cell.

Saturation constraint

The saturation constraint is

$$\sum_{j=1}^{n_p} S_j = 1 \qquad \textbf{(43)}$$

Phase pressures

The phase pressure is related to the capillary pressure and a reference pressure, P_{ref}:

$$P_j = P_{ref} + P_{cref,j} \text{ for } j = 1,....,n_p \qquad \textbf{(44)}$$

For n_p phases, there are (n_p-1) independent capillary equations. The capillary pressure is a function of phase saturations and compositions,

$$P_{cref,j} = P_{cref,j}(\vec{S}, \vec{x}) \qquad \textbf{(45)}$$

for $j = 1,....,n_p$

Formation porosity

The porosity is a function of pressure.

$$\phi = \phi_{ref}(1 + c_f(P - P_{ref})) \qquad \textbf{(46)}$$

where ϕ_{ref} is the porosity at the reference pressure, P_{ref} *and* ϕ is calculated at the pressure *P*.

In GPAS, the porosity calculation is performed in the subroutine AQUEOUS. The AQUEOUS subroutine also calculates the aqueous phase molar and mass densities.

Physical property models

In this section, the physical models implemented in GPAS to calculate the viscosities, interfacial tension, relative permeability, capillary pressure, phase molar density and the hydrocarbon solubility in water are described.

Viscosity

The aqueous phase viscosity is constant and is specified as user input. The gas and oil viscosity computed using the Lohrenz et al. (1964) correlation. An option is also available to input the oil phase viscosity. All the phase viscosity calculations are performed in the subroutine VIS, which consists of the subroutines LVISC1 and LVISC2. LVISC1 subroutine computes the viscosity of pure components at low pressures while LVISC2 subroutine computes the viscosity of a mixture and its derivatives with respect to phase composition and pressure at high pressures.

Lohrenz et al. Correlation

The Lohrenz et al. (1964) correlation combined several viscosity correlations. The steps involved in calculating the phase viscosity are given below:

- Computation of the low-pressure, pure-component viscosity:

$$\widehat{\mu}_i = \frac{0.00034 T_{ri}^{0.94}}{\varsigma_i} \text{ for } T_{ri} \le 1.5$$

or

$$\widehat{\mu}_i = \frac{0.0001776(4.58T_{ri} - 1.67)^{5/8}}{\varsigma_i} \text{ for } T_{ri} > 1.5 \qquad \textbf{(47)}$$

where

$$\varsigma_i = \frac{5.44 T_{ci}^{1/6}}{MW_i^{1/2} P_{ci}^{2/3}}$$

- Calculation of the low pressure viscosity :

$$\mu_j^* = \frac{\sum_{i=1}^{n_c} x_{ij}\hat{\mu}_i\sqrt{MW_i}}{\sum_{i=1}^{n_c} x_{ij}\sqrt{MW_i}} \quad \textbf{(48)}$$

- The reduced phase molar density calculation

$$\xi_{jr} = \xi_j \sum_{i=1}^{n_c} x_{ij} V_{ci} \quad \textbf{(49)}$$

$$\eta_j = \frac{5.44\left[\sum_{i=1}^{n_c} x_{ij}T_{ci}\right]^{1/6}}{\left[\sum_{i=1}^{n_c} x_{ij}MW_i\right]^{1/2}\left[\sum_{i=1}^{n_c} x_{ij}P_{ci}\right]^{2/3}}$$

- The Phase viscosity calculation at the desired pressure

$$\mu_j = \mu_j^* + 0.000205\frac{\xi_{jr}}{\eta_j} \text{ for } \xi_{jr} \le 0.18$$

$$\mu_j = \frac{\mu_j^* + (\chi_j^4 - 1)}{10^4\eta_j} \text{ for } \xi_{jr} > 0.18 \quad \textbf{(50)}$$

where

$$\chi_j = 1.023 + 0.23364\xi_{jr} + 0.58533\xi_{jr}^2 - 0.40758\xi_{jr}^3 + 0.093324\xi_{jr}^4$$

Interfacial Tension

The interfacial tension between two hydrocarbon phases is calculated from the Macleod-Sudgen correlation as reported in Reid, Prausnitz and Poling (1987):

$$\sigma_{jl} = \left[0.016018\sum_{i=1}^{n_c}\psi_i(\xi_j x_{ij} - \xi_l x_{il})\right]^4 \quad \textbf{(51)}$$

where ψ_i is the parachor of component i.

In GPAS, the interfacial tension between gas and oil for gridblock k and the derivatives of the interfacial tension are calculated in the subroutine IFT.

Relative Permeability

The two-phase relative permeability is given as tabular input. The three -phase relative permeability to water, oil and gas is calculated based on the two-phase relative permeability data using Stone's method I or II.

Stone's Model II

The three-phase oil relative permeability is calculated from the two-phase relative permeability using

$$k_{r2} = k_{r2}^{0}\left[\left(\frac{k_{r21}}{k_{r2}^{0}} + k_{r1}\right)\left(\frac{k_{r23}}{k_{r2}^{0}} + k_{r3}\right) - \left(k_{r1} + k_{r3}\right)\right] \qquad \textbf{(52)}$$

where the oil/water and oil/gas two-phase relative permeability is obtained from the input tables.

The subroutine RELPERM3EOS computes the three-phase relative permeability to water, oil and gas based on the two-phase data.

Capillary Pressure

The gas-oil and water-oil capillary pressure data are inputted as tables. The capillary pressure at any saturation is interpolated from the tables.

Hydrocarbon Solubility in Water

The solubility of the hydrocarbons in the water is calculated, separately from the flash calculations, using Henry's law. The vaporization of water into hydrocarbon phases is ignored. When the solubility calculations are treated separately from the flash calculations, the component molar balance equations are expressed as

$$\frac{\partial(N_i^h + N_i^a)}{\partial t} - \overline{\nabla} \bullet \sum_{j=1}^{n_p} \xi_j \lambda_j x_{ij} (\vec{\nabla} P_j - \gamma_j \vec{\nabla} D) - \frac{q_i}{V_b} = 0 \qquad \textbf{(53)}$$

where N_i^h is the moles of component i in the hydrocarbon phase, N_i^a is the moles of component i in the aqueous phase and i is each hydrocarbon component.

N_i^h is selected as the primary variable instead of the total number of moles. The solution approach is identical to that outlined earlier in the solution procedure with the

exception that the solubility of hydrocarbon components in the aqueous phase needs to be determined using the unknowns during the Newton iterations of the governing equations. This is done as follows. In step 2 of the solution procedure given in the next section, the solubility of each component in the aqueous phase is calculated using Henry's law.

$$x_i^a = \frac{f_i^a}{H_i} = \frac{N_i^a}{N_w^a + \sum_{i=1}^{n_c} N_i^a} \qquad \textbf{(54)}$$

The mole fraction of water in the aqueous phase is

$$x_w^a = 1 - \sum_{i=1}^{n_c} x_i^a = \frac{N_w^a}{N_w^a + \sum_{i=1}^{n_c} N_i^a} \qquad \textbf{(55)}$$

Dividing Equation **54** by Equation **55** yields

$$N_i^a = \frac{x_i^a}{x_w^a} N_w^a \qquad \textbf{(56)}$$

Since N_i^a can be determined using the primary variables as shown in the above equation, it is apparent that the inclusion of the solubility calculations doesn't increase the number of primary variables.

Well model

The well model accounts for the source/sink terms in the mass conservation equations. A reservoir simulator needs a well model to translate historical production/injection data and the actual or desired field operating conditions and constraints into acceptable controls for the reservoir model. This requires that the operating constraints such as production and injection facility limits be imposed correctly as boundary conditions for the individual gridblock representing part or all of a well in the reservoir model. The well-management routine assigns user-specified well rates or pressures to individual producing blocks in the simulator at specified times. The application of a constant-pressure boundary condition will hold the bottom hole

production or injection pressure in the well constant. A well is located at the center of the gridblock containing the well. The equations given below apply only for vertical wells.

The relationship between volumetric flow rate, flowing bottom hole pressure and gridblock pressure is expressed as

$$Q_j = PI_j(P_{wf} - P_j) \quad \textbf{(57)}$$

where PI_j is the productivity index for phase j. For one-dimensional (x-direction) and x-z cross-sectional simulations, the productivity index is given by (Chang, 1990):

$$PI_j = \frac{\sqrt{k_x k_y}\,\Delta y \Delta z \lambda_{rj}}{25.15 * 2\pi\left(\frac{\Delta x}{2}\right)} \quad \textbf{(58)}$$

For two-dimensional areal and three-dimensional simulations, the phase productivity index is computed as

$$PI_j = \frac{\sqrt{k_x k_y}\,\Delta z \lambda_{rj}}{25.15 \ln\left(\frac{r_o}{r_w}\right)} \quad \textbf{(59)}$$

where k_x and k_y (md) are permeability in the x and y directions, Δx, Δy and Δz are gridblock sizes (ft) in x,y and z directions, λ_{rj} is relative mobility in cp^{-1}, Q_j is the well flow rate of phase j in ft^3/day and pressure is in psi. In Equation **59**, the radius r_o is given by Peaceman's equation:

$$r_o = 0.28 \frac{\left[\left(\frac{k_x}{k_y}\right)^{1/2}\Delta x^2 + \left(\frac{k_x}{k_y}\right)^{1/2}\Delta y^2\right]}{\left(\frac{k_y}{k_x}\right)^{1/4} + \left(\frac{k_x}{k_y}\right)^{1/4}} \quad \textbf{(60)}$$

Constant bottomhole flowing pressure injector

The bottomhole flowing pressure at elevation z is calculated from this reference pressure as follows:

$$(P_{wf})_z = P_{bot} - \gamma_{inj}(z - z_{bot}) \quad \textbf{(61)}$$

where γ_{inj} is the specific weight of the injected fluid at the well pressure. The bottomhole reference depth for each well can be assigned in the input file.

The component flow rates for layer z are computed by

$$(q_i)_z = \left[1-(f_1)_{inj}\right](z_i)_{inj}(q_t)_z \qquad \textbf{(62)}$$

for $i = 1,....,n_c$

$$(q_{n_c+1})_z = (f_1)_{inj}(q_t)_z \qquad \textbf{(63)}$$

and

$$(q_t)_z = \frac{(Q_t)_z}{(v_t)_{inj}} \qquad \textbf{(64)}$$

where

$$(Q_t)_z = \sum_{j=1}^{n_p}(PI_j)_z\left[(P_{wf})_z - (P_j)_z\right] \qquad \textbf{(65)}$$

And

$$(v_t)_{inj} = \left(\frac{f_1}{\xi_1}\right)_{inj} + \left[\left(1-(f_1)_{inj}\right)\right]\left[\left(\frac{L_2}{\xi_2}\right)_{inj} + \left(\frac{L_2}{\xi_2}\right)_{inj}\right] \qquad \textbf{(66)}$$

where $(\xi_j)_{inj}$ is the molar density of phase j, $(L_j)_{inj}$ is a ratio of moles in hydrocarbon phase j to the total number of hydrocarbon moles in the injection fluid and $(f_1)_{inj}$ is the molar fraction of water component in the injection stream. The values of $(\xi_j)_{inj}$ and $(L_j)_{inj}$ for j = 2 and 3 are determined by flash calculations at the time the well conditions are specified. The molar density for the aqueous phase, which is assumed to be slightly compressible, is calculated using

$$\xi_1 = \xi_1^o\left[1 + c_1(P - P_1^o)\right] \qquad \textbf{(67)}$$

where ξ_1^o is the aqueous phase molar density at the reference pressure P_1^o.

Constant bottomhole flowing pressure producer

The flowing bottomhole pressures for a layer z is calculated using

$$(P_{wf})_z = P_{bot} - \gamma_z(z - z_{bot}) \qquad \textbf{(68)}$$

The layer component flow rate is found by

$$(q_i)_z = \sum_{j=2}^{n_p} (\xi_j x_{ij} PI_j)_z (P_{wf} - P_j)_z \qquad \textbf{(69)}$$

for $i = 1,....,n_c$

And

$$(q_{n_c+1})_z = (\xi_1 PI_1)_z (P_{wf} - P_1)_z \qquad \textbf{(70)}$$

In GPAS, the main well model calculations are done in the subroutine XWELL, which calls the subroutines WELLRATE and PRDWDEN. The WELLRATE subroutine calculates the molar flow rates and volumetric flow rates of each component in each layer and for each well. At present, only the constant bottomhole flowing pressure constraint is implemented. The productivity index is calculated in the subroutine IWELL. The wellbore fluid density for production wells required to calculate the flowing well production pressure at each layer is computed in the subroutine PRDWDEN.

Overall computation procedure of the simulator

Primary and secondary variables

The independent variables for solving the governing equations are

$P, N_1, N_2,...., N_{n_c}, \ln K_1, \ln K_2,....., \ln K_{n_c}$

The equilibrium ratio, K_i is defined as

$$K_i = \frac{y_i}{x_i} \qquad \textbf{(71)}$$

where x_i and y_i are the mole fractions of component i in oil and gas phases, respectively.

The set of the independent variables is further classified into the primary and secondary variables. The primary variables are $P, N_1, N_2,...., N_{n_c}$ because they are coupled between adjacent cells through the component mass-balance equations and need to be solved simultaneously. The $\ln K$ values are the secondary variables because they are calculated from the equality of the component fugacities at given pressure, temperature and total moles of all components.

Solution procedure

A fully implicit solution method is used to solve the governing equations. The equations are nonlinear and must be solved iteratively. A Newton procedure is used in which the system of nonlinear equations is approximated by a system of linear equations. The Jacobian term refers to the matrix whose elements are the derivatives of the governing equations with respect to the independent variables.

The sequence of steps involved in the solution of the governing equations for the independent variables over a timestep include:

1. *Initialization in each gridblock* : The Pressure, overall composition and temperature of the fluids in each gridblock are specified.

   The initialization and calculation of the initial fluid in place is done in the subroutine INFLUID0. This subroutine is the main driver for the computation of the initial fluid in place.

2. *Phase identification and Physical properties calculation*: The flash calculations are performed in each gridblock and the phase saturations, compositions and densities are determined. The phases are then identified as gas, oil or aqueous phase. Phase viscosities and relative permeabilities are subsequently computed. The flash calculations are performed in the subroutine XFLASH and currently are limited to two phases. The Rachford-Rice equation that determines the phase fractions is coded in the subroutine SOLVE. All the fluid physical properties like the fluid viscosity, relative permeability and phase density calculations are determined in the PROP subroutine. The PROP subroutine calls separate routines to determine the different physical properties. It calls the subroutine LVISC2 to calculate the phase viscosity using the Lorenz coefficient, the subroutine RELPERM3EOS to calculate the three-phase relative permeability using Stone's model or calls the LOOKUP

subroutine to interpret the two-phase relative permeability from the relative permeability tables.

3. *Governing Equations Linearization*. All the governing equations are linearized in terms of the independent variables and the elements of the Jacobian are calculated.

   The subroutine JACOBIAN that in turn calls PREROW generates the Jacobian for the linear system. PREROW is the main subroutine that calls the other subroutines, each with a specific task of computing the derivatives of separate equations and terms. The subroutine JACCUM calculates the derivatives of the accumulation term of the component balance. The subroutine JACO2 calculates the derivatives related to transmissibility terms. The subroutine JMASS calculates the derivatives related to the component mass balance in X, Y and Z directions. The derivatives of the source/sink terms are calculated in JSOURCE.

4. *Jacobian Factorization and reduction of the linear systems.* A row elimination is performed to reduce the size of the linear system from $2n_c + 1$ to n_c for each gridblock. To achieve this, the linearized phase-equilibrium relations and the linearized volume constraint are used to eliminate the secondary variables and one of the overall component moles from the linearized component mass balance equations.

   The subroutine EOS_JACO forms the jacobian for row elimination for two-phase cells.

5. *Solution of the reduced system of the linear equations for the primary variables.* The reduced system of linear equations is simultaneously solved for pressure and the overall moles of $n_c - 1$ components per unit bulk volume for all the cells.

6. *Secondary variables calculation.* A back substitution method is

employed to compute the secondary variables $\ln K$ and overall moles of the component eliminated in Step 4 using the factorized Jacobian. The phase-stability analysis is then carried out for all the gridblocks using the newly updated pressure and overall component moles.

7. *Updating phase densities and viscosities, determination of single-phase state and estimation of phase relative permeability.*

   The subroutine XUPDATE updates the phase composition and the phase properties as phase density, viscosity, relative permeability and determination of single phase in each cell. The main subroutine in the compositional model EOSCOMP is XSTEP. XSTEP calls XDELTA, which in turn calls the XUPDATE subroutine.

8. *Check for convergence.* The residuals of the linear system obtained in step 3 are used to determine convergence. If a tolerance is exceeded, the elements of the Jacobian and the residuals of the governing equations are then updated and another Newton iteration is performed by returning to Step 4. If the tolerance is met, a new timestep is then started by returning to Step 3.

   The subroutine XSTEP is the contact routine between the IPARS framework code and the EOSCOMP compositional model code. The residuals are checked in XSTEP and if the tolerance is met, a new timestep is started, else another newton iteration is performed.

Executive routines in EOSCOMP

The executive routines in the EOSCOMP model are as follows:

XISDAT — All the initial scalar data are read by this subroutine. These include the physical properties of each component, default number of iterations, convergence tolerances for a variety of

	calculations, output flags, operation specific flags and chemical property data. No grid-element arrays can be reference in this subroutine.
XARRAY	This subroutine allocates memory for all the grid element arrays
XIADAT	The entire grid element array input as the pressure, water saturation, feed composition is read in and written out to a file
XIVDAT.	Performs the model initialization before time iteration. The PETSc linear solver is also initialized.
XSTEP	The main subroutine that performs all the calculations over a timestep.
XQUIT	Exits from the simulation when it meets the maximum time, production limits, or if an error occurs.

The communication between processors for the compositional model is performed in the executive subroutines. There is no argument attached to these calls. Those variables associated with grids are passed into these routines through pointers that are stored in common block. These common blocks are included as header files in the subroutines. The executive routines call the work routines to perform all the calculations. The grid dimensions and variables are passed into these work routines through a C routine called CALLWORK, which is handled by the framework. The CALLWORK function passes the variables as an index argument list to the function being called.

Description of the Solver

PETSc (Balay *et al.*, 1997, 1998; Wang *et al.*, 1999) is a large suite of parallel, general-purpose, object-oriented solvers for the scalable solution of partial differential equations discretized using implicit and semi-implicit methods. PETSc is implemented in C, and is usable from C, Fortran, and C++. It uses MPI for communication across

processors. GPAS uses the linear solver component of PETSc to solve the linearized Newton system of equations and uses the parallel data formats provided by PETSc to store the Jacobian and the vectors.

The linear solver components of PETSc provides a unified interface to various Krylov methods, such as conjugate gradient (CG), generalized minimal residual (GMRES), biconjugate gradient, etc. and also to various parallel preconditioners such as Jacobi, block preconditioners like block Jacobi, domain decomposition preconditioners like additive Schwartz. GPAS uses the biconjugate gradient stabilized approach as the Krylov method and block Jacobi preconditioner, with point block incomplete factorization (ILU) on the subdomain blocks. The point block refers to treating all the variables associated with a single gridblock as a single unit. The number of subdomain blocks for block Jacobi is chosen to match the number of processors used, so that each processor gets a complete subdomain of the problem and does a single local incomplete factorization on the Jacobian corresponding to this subdomain.

For three-phase flow, the compositional model. EOSCOMP generates $2n_c+1$ equations per gridblock, causing the Jacobian to have a point-block structure and a point-block sparse storage format is used to store the matrix. These $2n_c+1$ equations do not result in complete coupling of all the variables across gridblocks. This causes the Jacobian to have some n_c+1 point-block locations with zero values. Thus a block size of n_c+1 is chosen for this matrix type eliminating the need to store the $(n_c+1)\ (n_c+1)$ blocks with zero values. The usage of the point-block sparse matrix storage lead to the improvement in the performance of the matrix routines.

Task 2: Formulation and Implementation of Chemical Module

The first set of chemical species added to the GPAS simulator is the tracer. Thus, although all the formulation in the aqueous species modeling applies to tracer, polymer and surfactant, each of these species modeling can involve, in addition, its own assumptions, formulations and special properties. Henceforth, the aqueous species refers to a species present in trace quantities in the aqueous phase and this includes a tracer, polymer or surfactant, the main subroutine XAQCOMP solving for the aqueous species concentration as a function of space and time is referred as the chemical subroutine and the whole module encompassing all the separate subroutines modeling the tracer, polymer and surfactant features is referred as the chemical module. The final output of the chemical subroutine XAQCOMP is the dimensionless aqueous species concentration, which also applies as the physical tracer concentration.

In GPAS simulator, the chemical module was linked to the equation-of-state compositional model EOSCOMP in an explicit manner. After EOSCOMP solves for the pressures, saturations and compositions of the non-aqueous species components for a particular time step and the convergence for the mass balance equations is attained, the chemical subroutine imports the required input from the host EOSCOMP and solves for the aqueous species mass balance equation to find the concentration at a given point in space and time.

This decoupled approach is more computationally efficient than solving all of the equations simultaneously in EOSCOMP.

Maroongroge (1994) used the following approach for tracer calculations in UTCOMP:

- Solution of the pressure equation.
- Solution of the mass conservation equations for species other than tracers

- Flash calculation to calculate the phase compositions of species other than tracers.
- Computation of the phase densities, saturations, relative permeabilities, and capillary pressures.
- Solution of the mass conservation equations for tracer components from the independent variables. This includes the re-determination of the upstream locations from the potentials, the calculation of the convection terms from the transmissibility coefficients, phase mole fractions, densities and fluxes, and the recalculation of the well flow rates in each layer.
- Return to the first step, the solution of the pressure equation for a new time step.

In GPAS, the parameters such as the phase flux, phase saturation, phase density and upstream locations are already being calculated in EOSCOMP. Because the aqueous species do not alter the phase behavior, the equation-of-state flash calculations are performed only for the non-aqueous species and subsequently the phase saturations, phase densities and phase fluxes are determined. In order to make the code efficient, these fluid flow and rock parameters were transferred from EOSCOMP at the last Newtonian iteration of each timestep to the chemical subroutine. The grid-block pressures are no longer required as the other parameters have already accounted for the pressure term.

The simplified method used in GPAS is as follows:

- Transfer of phase saturations, phase densities, phase flux, upstream locations and the well molar flow rates from EOSCOMP to the chemical subroutine.
- Solution of the mass conservation equation for the aqueous species incorporating the convection terms and the source/sink terms.
- Return to Step 1 for a new time step

A notable feature of this method is that the chemical module calculations are not performed for each Newtonian iteration in a timestep, since the equations for aqueous species flow are decoupled and can be solved explicitly. This saves considerable computing time for reservoir simulations with a large number of gridblocks.

Mathematical formulation

Aqueous Species Mass Conservation Equation

The differential form for the species mass conservation equation is expressed as:

$$\frac{\partial}{\partial t}\left(\phi\sum_{j=1}^{Np}\rho_j S_j \omega_{ij} + (1-\phi)\rho_s \omega_{is}\right) + \vec{\nabla}\bullet\left(\sum_{j=1}^{Np}(\rho_j \omega_{ij}\overrightarrow{u_j} - \phi S_j \rho_s \overrightarrow{\overrightarrow{K_{ij}}}\bullet\vec{\nabla}\omega_{ij})\right) \qquad \textbf{(2.1)}$$
$$= R_i, i = 1,..,Nc$$

where ρ_j is the mass density of phase j, S_j is the saturation of phase j, ω_{ij} is the mass fraction of species i in j, ρ_s is the mass density of the stationary phase s, $\overrightarrow{\overrightarrow{K_{ij}}}$ is the dispersion tensor, ω_{is} is the mass fraction of species i in the stationary phase s, $\overrightarrow{u_j}$ is the flux of phase j, and R_i is the source/sink term.

The species mass conservation equation was simplified to model the aqueous species flow using the below assumptions:

- Aqueous species do not occupy any volume
- Physical dispersion is neglected.
- Radioactive decay does not occur
- Aqueous species stay in the aqueous phase and do not partition to the oil or gas phase.

The additional specific assumptions that apply only to a physical tracer are

- Tracers do not change the physical properties of the fluids.
- Tracer adsorption does not take place
- Tracers do not undergo chemical reactions

Thus, the surfactant and polymer component modeling option will include the capability of a surfactant and polymer to change the physical properties of the fluids, to adsorb on the rock surfaces and to undergo chemical reactions. But these surfactant and polymer specific features are added as adjunct subroutines and thus they do not change the aqueous species flow modeling equation. Thus the assumptions of a tracer flow can be applied to the aqueous species flow equation.

Applying these assumptions, the mass conservation Equation **2.1** reduces to:

$$\frac{\partial}{\partial t}\left(\phi\rho_1 S_1 \omega_{i1}\right) + \vec{\nabla} \bullet \left(\rho_1 \omega_{i1} \vec{u_1}\right) = R_i \qquad \textbf{(2.2)}$$

The above differential equation was discretized as follows:

$$\left\{\frac{\left(\phi^{n+1}\rho_1^{n+1}S_1^{n+1}\right)w_{i1}^{n+1} - \left(\phi^{n}\rho_1^{n}S_1^{n}\right)w_{i1}^{n}}{\Delta t}\right\} = \qquad \textbf{(2.3)}$$

$$-\left\{\frac{\left(\rho_1^{n+1}U_{x1}^{n+1}w_{i1}^{n}\right)_{x+1/2} - \left(\rho_1^{n+1}U_{x1}^{n+1}w_{i1}^{n}\right)_{x-1/2}}{\Delta x}\right\}$$

$$-\left\{\frac{\left(\rho_1^{n+1}U_{y1}^{n+1}w_{i1}^{n}\right)_{y+1/2} - \left(\rho_1^{n+1}U_{y1}^{n+1}w_{i1}^{n}\right)_{y-1/2}}{\Delta y}\right\}$$

$$-\left\{\frac{\left(\rho_1^{n+1}U_{z1}^{n+1}w_{i1}^{n}\right)_{z+1/2} - \left(\rho_1^{n+1}U_{z1}^{n+1}w_{i1}^{n}\right)_{z-1/2}}{\Delta z}\right\}$$

$$+\frac{\left(\rho_1^{n+1}q_1^{n+1}\right)w_{i1,inj}}{V_b^{n+1}}$$

The one point upstream weighting method is used in this finite-difference formulation. In the absence of the physical dispersion, all the dispersion in the tracer output is contributed by the numerical dispersion. The upstream locations and the phase fluxes are transferred from the subroutine MRESIPW and the wellflow rates are obtained from the subroutine XWELL.

We are in the process of implementing and testing of the tracer option.

Task 3: Validation and Application

Test cases were run on GPAS and the results were compared with both analytical solutions and output from the miscible-gas flooding compositional simulator, UTCOMP (Chang, 1990), or the chemical flooding simulator, UTCHEM (Delshad et al., 1996), to check the correctness of the code. The flash algorithm was tested with a batch flash calculation for a binary mixture. A Buckley-Leverett problem was run on GPAS and compared with the analytical solution and output from the chemical flooding simulator UTCHEM. A comparison of the results from GPAS with UTCOMP of an example simulation of carbon dioxide sequestration is also given. The standard SPE fifth comparative solution project (Killough and Kossack, 1987) was modified and simulations were carried out on GPAS and UTCOMP. The comparison of these results from GPAS with UTCOMP for the modified SPE fifth comparative solution project is discussed.

Batch flash of Ethane-Propylene binary mixture

The goal is to verify the correctness of the flash calculations. The mathematical formulation of the flash algorithm is discussed in Task 1. The test case considered here is a mixture of ethane and propylene. The simulation domain dimensions are 5000 ft in length, 500 ft in width and 20 ft in thickness. Since the simulation is a batch flash, there is no well section in the input. The initial composition is 0.5 mole fraction each of ethane and propylene. The details of the input file including the critical properties of the components are given in **Table 3.1**. The simulation is run for one day. A program for multi-component vapor-liquid equilibrium calculations using the Peng-Robinson cubic equation-of-state, VLMU (Sandler, 1999) was also used as a basis for comparison.

UTCOMP and GPAS use the same form of PR EOS while VLMU uses a slightly different form of PR EOS. For acentric factor values less than 0.49, all the three codes use the same equations. The only difference is that GPAS and UTCOMP use a different expression for the calculation of κ (Equation **29**) for the acentric factor values greater

than 0.49 while VLMU uses the same expression for all values of acentric factors (Equation **28**). Since in this test case, the acentric factor for both the components is less than 0.49, all the three codes essentially use the same PR EOS equations. The iteration tolerances in UTCOMP and GPAS are set at 10^{-8}. The volume shift parameter functionality is available in UTCOMP but is not implemented in GPAS and VLMU. Hence the volume shift parameter is taken as zero in UTCOMP.

Changing the binary interaction coefficient to 0, 0.01 and 0.05, three simulation runs were made. The oil and gas phase compositions from GPAS, UTCOMP and VLMU are compared in **Table 3.2**. The differences in the concentrations were based on VLMU solution. The oil and gas phase molar densities obtained from GPAS and UTCOMP are compared in **Table 3.3**. A reasonable agreement was obtained for the flash calculation results between GPAS and UTCOMP.

Buckley Leverett 1-D water flood

The Buckley-Leverett problem was chosen as a test problem because there is an analytical solution available for comparison. This problem often serves as a test for new numerical methods and as a building block of simulation models involving simultaneous flow of immiscible fluids in porous media.

The problem considered is a one-dimensional waterflood in a gas free, homogenous, isotropic reservoir. The homogenous permeability is 500 md. The simulation domain extends to 400 ft in the x direction, 1 ft in the y direction and 1 ft in the z direction. A 40x1x1 grid was used for this run. The initial water saturation in the reservoir is 0.1. The only injector is located at gridblock (1,1,1) and the only producer is located at gridblock (40,1,1). The initial reservoir pressure is 1500 psia. Water is injected at a constant bottom hole pressure of 2000 psia and the producer is maintained at a constant bottom hole pressure of 1500 psia. The relative permeability curves used for this problem are shown in **Figure 3.1**. The two-phase relative permeability tables, used

in GPAS, were generated based on these functions. The end point mobility ratio is 3.15. The reservoir description, the hydrocarbon component properties and the time step details of the input file are given in **Table 3.4**. The fractional flow curves of oil and water are presented in **Figure 3.2**. The water saturation profile results from GPAS, at different injected pore volumes, was compared with the output from UTCHEM and the analytical solution in **Figure 3.3** The one-point upstream weighting numerical method is employed for this simulation in GPAS, while both one point upstream and third order TVD (total variation diminishing) methods are employed in UTCHEM. A constant time step of 0.1 days in used in UTCHEM while in GPAS the maximum time step is 0.0005 days and the minimum time step is 0.00001 days. When the third order TVD numerical method (total variation diminishing) is used in UTCHEM, its results are closer to the analytical solution than when the one point upstream weighing method is used.

Carbon dioxide sequestration case

The injection of carbon dioxide into a two-dimensional, isotropic, homogenous aquifer was simulated. After making the simulations with GPAS and UTCOMP, the pressure, saturation and composition profiles were compared.

The simulation domain is 500 ft in length, 500 ft in width and 100 ft in thickness. A 5x5x1 grid was used for this simulation. Water is treated here as a component so that the solubility of the carbon dioxide in the liquid water phase can be calculated from the equation-of-state. Phase 2 is the active liquid water phase and phase 3 is the gas phase in these simulations. The usual water phase is 1, but it plays no significant role in these simulations. Its saturation was a constant equal to 0.2. Carbon dioxide is injected into the aquifer through the injector located at gridblock (1,1,1) at a bottom hole pressure of 2000 psi. The producer well is located at gridblock (5,5,1) with a constant bottom hole pressure of 1000 psi. The initial reservoir pressure is 1500 psi. **Figure 3.4** shows a diagram of the reservoir. A summary of the input data is given in **Table 3.5**.

The simulation is carried out for 100 days and the pressure, the saturation and composition profiles at the end of 100 days compared with good agreement. The pressure profile along the x-axis has been plotted for every Y index in **Figure 3.5**. The gas saturation profile along the x-axis was plotted for every Y grid index in **Figure 3.6**. The compositions of the water phase and the gaseous phase at the end of 100 days from GPAS and UTCOMP are given in **Table 3.6**. The absolute differences between the compositions obtained from GPAS and UTCOMP at the end of 100 days are given in **Table 3.7**.

Six-Component compositional simulation example

This test is a modified version of the SPE fifth comparative solution problem. The hydrocarbon phase consists of six components. The hydrocarbon component critical properties are given in **Table 3.8**. Two-dimensional and three-dimensional simulations of the same problem were run to verify the correctness of the two- and three-dimensional features of the simulator.

Two Dimensional Quarter Five Spot Case

A quarter five spot pattern (5x5x1) is used for this run. The reservoir description and the well constraints are presented in **Table 3.9**. The simulation domain comprises of 500 ft in the x direction, 500 ft in the y direction and 100 ft in the z direction. The injector well is located at (1,1,1) and the producer well is located at (5,5,1). Gas is injected into the reservoir and it pushes the oil towards the producer. The water phase is immobile. The pressure profile and the saturation profile at the end of 100 days obtained from GPAS and UTCOMP was compared and a good agreement was obtained. The pressure profile along the x-axis has been plotted for every Y index in **Figure 3.7**. The oil saturation profile and the gas saturation profile along the x-axis for every y index is plotted in **Figure 3.8** and **Figure 3.9** respectively and as shown there is a reasonably

good agreement obtained between the two simulator results. This supports the correctness of the two dimensional three phase compositional capabilities of GPAS.

Three Dimensional Case

A 10x10x5 finite difference grid was used as shown in **Figure 3.10**. The input data summary for this run is given in **Table 3.10**. The critical properties and the binary interaction coefficients are given in **Table 3.8**. The injector well and the producer well are completed through all the five layers. The injector is located at (1,1) and the producer well is located at (10,10). Gas is continuously injected at a constant bottomhole pressure of 1700 psi and the producer well is constantly maintained at 1300 psi. The initial reservoir pressure is 1500 psi. The water phase is immobile. The test case is run on GPAS and UTCOMP for a simulation period of two years. The pressure distribution, fluid saturations and concentrations from GPAS compared well with UTCOMP. The plots of the pressure profile along the x axis for the even grid index in the Y direction and only for the top layer at the end of two years is plotted in **Figure 3.11**. The oil saturation profile and the gas saturation profile along the x-axis, only for the extreme Y grid index in the top layer and at the end of two years, from GPAS and UTCOMP were compared in **Figure 3.12** and **Figure 3.13** respectively. The average reservoir pressure history from GPAS and UTCOMP were compared in **Figure 3.14**. The overall production gas oil ratio comparison plots are shown in **Figure 3.15.**

Table 3.1: Summary of input data for the ethane-propylene mixture batch-flash calculation.

Dimensions (ft):	Length	5000
	Width	500
	Thickness	20
Porosity (fraction)		0.35
Permeability (md)		0.001
Reservoir Temperature (^oF)		100
Initial Reservoir Pressure (psi)		435.11
Initial Composition (mole fraction)	C_2H_6	0.5
	C_3H_6	0.5
Simulation Time (day)		1.0
Time Step Size (day)		0.1

Component Critical Properties:

Component	T_c (^0R)	P_c (psi)	V_c (ft^3/lb-mole)	ω_i (dyne$^{1/4}$ cm$^{11/4}$/gm-mole)	MW_i (lbm/lb-mole)	ψ_i
C_2H_6	549.72	708.36	2.3703	0.098	30.070	111
C_3H_6	657.00	670.07	2.899	0.148	42.081	40.0

Binary Interaction Coefficients:

Component	C_2H_6	C_3H_6
C_2H_6	0	0
C_3H_6	0	0

Binary Interaction coefficient	Component Concentration (mole fraction)	VLMU	GPAS			UTCOMP		
		Final Composition	Solution	Absolute Difference	Difference Percentage	Solution	Absolute Difference	Difference Percentage
0	X C2H6	0.45	0.4496	0.0004	0.0888889	0.4468	0.0032	0.7111111
	Y C2H6	0.62	0.613	0.007	1.1290323	0.61005	0.00995	1.6048387
	X C3H6	0.55	0.5504	-0.0004	-0.072727	0.55332	-0.00332	-0.603636
	Y C3H6	0.38	0.387	-0.007	-1.842105	0.38995	-0.00995	-2.618421
0.01	X C2H6	0.4348	0.4399	-0.0051	-1.172953	0.43064	0.00416	0.9567617
	Y C2H6	0.6007	0.6001	0.0006	0.0998835	0.59667	0.00403	0.670884
	X C3H6	0.5651	0.5601	0.005	0.8847992	0.56936	-0.00426	-0.753849
	Y C3H6	0.3993	0.3999	-0.0006	-0.150263	0.40333	-0.00403	-1.009266
0.05	X C2H6	0.3701	0.3688	0.0013	0.3512564	0.36606	0.00404	1.0915969
	Y C2H6	0.55	0.549	0.001	0.1818182	0.54614	0.00386	0.7018182
	X C3H6	0.6299	0.6312	-0.0013	-0.206382	0.63398	-0.00408	-0.647722
	Y C3H6	0.45	0.451	-0.001	-0.222222	0.45386	-0.00386	-0.857778

X C2H6 concentration of Ethane in the oil phase
Y C2H6 concentration of Ethane in the gas phase
X C3H6 concentration of Propylene in the oil phase
Y C3H6 concentration of Propylene in the gas phase

Table 3.2: Comparison of the phase compositions from GPAS with UTCOMP and VLMU in the ethane propylene batch - flash test case.

Binary Interaction coefficient	GPAS		UTCOMP		ABSOLUTE DIFFERENCE	
	Oil Phase Molar Density (lbmol/ft3)	Gas Phase Molar Density (lbmol/ft3)	Oil Phase Molar Density (lbmol/ft3)	Gas Phase Molar Density (lbmol/ft3)	Oil Phase Molar Density (lbmol/ft3)	Gas Phase Molar Density (lbmol/ft3)
0	6.9762E-01	1.1366E-01	6.9702E-01	1.1360E-01	5.9721E-04	5.8230E-05
0.01	0.6949	0.1138	0.6943	0.1137	5.7580E-04	5.6940E-05
0.05	0.6864	0.1141	0.6859	0.1140	5.0027E-04	6.3020E-05

Table 3.3: Comparison of the phase molar densities from GPAS with UTCOMP and VLMU in the ethane propylene batch - flash test case

Table 3.4: Summary of input data for the one-dimensional Buckley Leverett Problem.

Dimensions (ft):	Length	400
	Width	1
	Thickness	1
Porosity (fraction)		0.25
Permeability (md)		500
Initial Water Saturation (fraction)		0.1
Reservoir Temperature (^{o}F)		130
Initial Reservoir Pressure (psi)		1500.
Initial Composition (mole fraction)	$C_{10}H_{22}$	1.0
Water viscosity (cp)		1.0
Oil viscosity (cp)		3.1527
Water Compressibility (1/psi)		$3.0x10^{-5}$
Rock Compressibility (1/psi)		0.0
Simulation Time (day)		75.0
Minimum Time Step Size in GPAS (day)		0.00001
Maximum Time Step Size in GPAS (day)		0.0005
Constant Time Step Size in UTCHEM (day)		0.00001
Injector Well Location (I,J,K)		(1,1,1)
Injection Bottomhole Pressure (psi)		2000
Injection Fluid Composition	$C_{10}H_{22}$	0.0
	H_2O	1.0
Producer Well Location (I,J,K)		(40,1,1)
Production Bottomhole Pressure (psi)		1500
Producer Well Location (I,J,K)		(40,1,1)
Production Bottomhole Pressure (psi)		1500

Table 3.4 (Cont.)

Component Critical Properties:

Component	T_c (^{0}R)	P_c (psi)	V_c (ft^3/lb-mole)	ω_i (dyne$^{1/4}$ cm$^{11/4}$/gm-mole)	MW_i (lbm/lb-mole)	ψ_i
$C_{10}H_{22}$	1111.8	304.0	12.087	0.488	142.3	431.0

Relative Permeability functions used for generating the tables

$K_{r1}^0 = 1$ $m = 4$ $S_{wr} = 0.1$	$K_{r2}^0 = 1$ $n = 4$ $S_{or} = 0$
$S = \frac{S_w - S_{wr}}{1 - S_{or} - S_{wr}}$ $K_{r1} = K_{r1}^o (S)^m$	$K_{r2} = K_{r2}^o (1 - S)^n$

Table 3.5: Summary of input data for the two dimensional carbon dioxide sequestration problem

Dimensions (ft):	Length	500
	Width	500
	Thickness	100
Porosity (fraction)		0.25
Permeability (md)		10
Initial Water Saturation (fraction)		0.2
Reservoir Temperature (^{o}F)		140
Initial Reservoir Pressure (psi)		1500
Initial Composition (mole fraction)	CO_2	0.002
	H_2O	0.998
Water viscosity (cp)		0.79
Water Compressibility (1/psi)		6.7e-5
Rock Compressibility (1/psi)		0.0
Simulation Time (day)		100.0
Constant Time Step Size (day)		0.1
Injector Well Location (I,J,K)		(1,1,1)
Injection Bottomhole Pressure (psi)		2000
Injection Fluid Composition	CO_2	0.999
Producer Well Location (I,J,K)		(5,5,1)
Production Bottomhole Pressure (psi)		1000

Table 3.5 (Cont.)

Component Critical Properties:

Component	T_c (^{0}R)	P_c (psi)	V_c (ft^3/lb-mole)	ω_i (dyne$^{1/4}$ cm$^{11/4}$/gm-mole)	MW_i (lbm/lb-mole)	ψ_i
CO_2	547.5	1071.0	1.505	0.23	44.01	49.0
H_2O	1165.14	3207.4	0.79890	0.34400	18.02	100.0

Binary Interaction Coefficients:

Component	CO_2	H_2O
CO_2	0	-0.085
H_2O	-0.085	0

Relative Permeability functions used for generating the tables

$$K_{r1} = 0.4089\left(\frac{S_1 - 0.2}{0.5}\right)^3$$

$$K_{r21} = \left(\frac{0.7 - S_1}{0.5}\right)^2$$

$$K_{r3} = 0.39\left(\frac{S_3 - 0.05}{0.6}\right)^3$$

$$K_{r23} = 0.83886\left(\frac{0.65 - S_3}{0.6}\right)^{2.1952}$$

Capillary Pressure functions used for generating the tables:

$$P_{c21} = 0.05 + 255.5328\exp(-8.689S_1)$$

$$P_{c23} = 6.00524x10^{-4}\exp(13.544618S_3)$$

GPAS RESULT

CO2 molefraction in the Mobile Water Phase

LX/LY(ft)	50	150	250	350	450
50	0.0215	0.0211	0.0207	0.0201	0.0049
150	0.0211	0.0208	0.0204	0.0134	0.0031
250	0.0207	0.0204	0.0193	0.0053	0.0024
350	0.0201	0.0134	0.0053	0.0029	0.0022
450	0.0049	0.0031	0.0024	0.0022	0.0021

H2O molefraction in the Mobile Water Phase

LX/LY(ft)	50	150	250	350	450
50	0.9785	0.9789	0.9793	0.9799	0.9951
150	0.9789	0.9792	0.9796	0.9866	0.9969
250	0.9793	0.9796	0.9807	0.9947	0.9976
350	0.9799	0.9866	0.9947	0.9971	0.9978
450	0.9951	0.9969	0.9976	0.9978	0.9979

CO2 molefraction in the Gas Phase

LX/LY(ft)	50	150	250	350	450
50	0.9808	0.9838	0.9863	0.9885	0
150	0.9838	0.9855	0.9875	0	0
250	0.9863	0.9875	0	0	0
350	0.9885	0	0	0	0
450	0	0	0	0	0

H2O molefraction in the Gas Phase

LX/LY(ft)	50	150	250	350	450
50	0.0192	0.0162	0.0137	0.0115	0
150	0.0162	0.0145	0.0125	0	0
250	0.0137	0.0125	0	0	0
350	0.0115	0	0	0	0
450	0	0	0	0	0

UTCOMP RESULT

CO2 molefraction in the Mobile Water Phase

LX/LY(ft)	50	150	250	350	450
50	0.021576	0.02113	0.020671	0.020119	0.004952
150	0.02113	0.020841	0.020395	0.013835	0.003108
250	0.020671	0.020395	0.019807	0.005362	0.002413
350	0.020119	0.013835	0.005362	0.002924	0.002178
450	0.004952	0.003108	0.002413	0.002178	0.002074

H2O molefraction in the Mobile Water Phase

LX/LY(ft)	50	150	250	350	450
50	0.97842	0.97887	0.97933	0.97988	0.99505
150	0.97887	0.97916	0.9796	0.98616	0.99689
250	0.97933	0.9796	0.98019	0.99464	0.99759
350	0.97988	0.98616	0.99464	0.99708	0.99782
450	0.99505	0.99689	0.99759	0.99782	0.99793

CO2 molefraction in the Gas Phase

LX/LY(ft)	50	150	250	350	450
50	0.98077	0.98388	0.98641	0.98853	0
150	0.98388	0.98566	0.98758	0	0
250	0.98641	0.98758	0.98938	0	0
350	0.98853	0	0	0	0
450	0	0	0	0	0

H2O molefraction in the Gas Phase

LX/LY(ft)	50	150	250	350	450
50	0.019229	0.01612	0.013588	0.011473	0
150	0.01612	0.014439	0.012419	0	0
250	0.013588	0.012419	0.010622	0	0
350	0.011473	0	0	0	0
450	0	0	0	0	0

Table 3.6: Comparison of the mobile water phase and gas phase compositions from GPAS with UTCOMP for the carbon dioxide sequestration problem.

Table 3.7: The absolute differences in the mobile water phase and gas phase compositions from GPAS with UTCOMP for the carbon dioxide sequestration problem at the end of 100 days.

ABSOLUTE DIFFERENCE IN VALUES BETWEEN GPAS AND UTCOMP RESULTS

CO2 molefraction in the Mobile Water Phase

LX/LY(ft)	50	150	250	350	450
50	-7.6E-05	-3E-05	2.9E-05	-1.9E-05	-5.2E-05
150	-3E-05	-4.1E-05	5E-06	-0.00044	-7.6E-06
250	2.9E-05	5E-06	-0.00051	-6.2E-05	-1.3E-05
350	-1.9E-05	-0.00044	-6.2E-05	-2.4E-05	2.17E-05
450	-5.2E-05	-7.6E-06	-1.3E-05	2.17E-05	2.56E-05

H2O molefraction in the Mobile Water Phase

LX/LY(ft)	50	150	250	350	450
50	8E-05	3E-05	-3E-05	2E-05	5E-05
150	3E-05	4E-05	0	0.00044	1E-05
250	-3E-05	0	0.00051	6E-05	1E-05
350	2E-05	0.00044	6E-05	2E-05	-2E-05
450	5E-05	1E-05	1E-05	-2E-05	-3E-05

CO2 molefraction in the Gas Phase

LX/LY(ft)	50	150	250	350	450
50	3E-05	-8E-05	-0.00011	-3E-05	0
150	-8E-05	-6E-05	-8E-05	0	0
250	-0.00011	-8E-05	-0.98938	0	0
350	-3E-05	0	0	0	0
450	0	0	0	0	0

H2O molefraction in the Gas Phase

LX/LY(ft)	50	150	250	350	450
50	-2.9E-05	8E-05	0.000112	2.7E-05	0
150	8E-05	6.1E-05	8.1E-05	0	0
250	0.000112	8.1E-05	-0.01062	0	0
350	2.7E-05	0	0	0	0
450	0	0	0	0	0

Table 3.8: Summary of the component critical properties and binary interaction coefficients for the two-dimensional six component simulation example.

Component Critical Properties:

Component	T_c (^{0}R)	P_c (psi)	V_c (ft^3/lb-mole)	ω_i (dyne$^{1/4}$ cm$^{11/4}$/gm-mole)	MW_i (lbm/lb-mole)	ψ_i
CH_4	343.0	667.8	1.599	0.013	16.0	71.00
C_3H_8	665.7	616.3	3.211	0.152	44.1	151.0
C_6H_{14}	913.4	436.9	5.923	0.301	86.2	271.0
$C_{10}H_{22}$	1111.8	304.0	10.087	0.488	142.3	431.0
$C_{15}H_{32}$	1270.0	200.0	16.696	0.650	206.0	631.0
$C_{20}H_{42}$	1380.0	162.0	21.484	0.850	282.0	831.0

Binary Interaction Coefficients:

Component	CH_4	C_3H_8	C_6H_{14}	$C_{10}H_{22}$	$C_{15}H_{32}$	$C_{20}H_{42}$
CH_4	0	0	0	0	0.05	0.05
C_3H_8	0	0	0	0	0.005	0.005
C_6H_{14}	0	0	0	0	0	0
$C_{10}H_{22}$	0	0	0	0	0	0
$C_{15}H_{32}$	0.05	0.005	0	0	0	0
$C_{20}H_{42}$	0.05	0.005	0	0	0	0

Table 3.9: Summary of input data for the two-dimensional six component simulation example.

Dimensions (ft):	Length	500
	Width	500
	Thickness	100
Porosity (fraction)		0.35
Permeability (md)		10
Initial Water Saturation (fraction)		0.2
Residual Water Saturation (fraction)		0.2
Reservoir Temperature (^{o}F)		160
Initial Reservoir Pressure (psi)		1500.
Initial Composition (mole fraction)	CH_4	0.5
	C_3H_8	0.03
	C_6H_{14}	0.07
	$C_{10}H_{22}$	0.2
	$C_{15}H_{32}$	0.15
	$C_{20}H_{42}$	0.05
Water viscosity (cp)		0.337
Water Compressibility (1/psi)		3.0e-6
Rock Compressibility (1/psi)		1.0e-6
Simulation Time (day)		100.0
Constant Time Step Size (day)		0.1
Injector Well Location (I,J,K)		(1,1,1)
Injection Bottomhole Pressure (psi)		2000
Injection Fluid Composition	CH_4	0.77
	C_3H_8	0.20
	C_6H_{14}	0.03
Producer Well Location (I,J,K)		(5,5,1)
Production Bottomhole Pressure (psi)		1000

Table 3.9 (Cont.)

Relative Permeability functions used for generating the tables

$$K_{r1} = 0.4089\left(\frac{S_1 - 0.2}{0.5}\right)^3$$

$$K_{r21} = \left(\frac{0.7 - S_1}{0.5}\right)^2$$

$$K_{r3} = 0.39\left(\frac{S_3 - 0.05}{0.6}\right)^3$$

$$K_{r23} = 0.83886\left(\frac{0.65 - S_3}{0.6}\right)^{2.1952}$$

Capillary Pressure functions used for generating the tables:

$$P_{c21} = 0.05 + 255.5328\exp(-8.689S_1)$$

$$P_{c23} = 6.00524x10^{-4}\exp(13.544618S_3)$$

Table 3.10: Summary of input data for the three-dimensional six component simulation example.

Dimensions (ft):	Length	500
	Width	500
	Thickness	150
Porosity (fraction)		0.35
Permeability (md)		10
Initial Water Saturation (fraction)		0.2
Residual Water Saturation (fraction)		0.2
Reservoir Temperature (^{o}F)		160
Initial Reservoir Pressure (psi)		1500
Initial Composition (mole fraction)	CH_4	0.5
	C_3H_8	0.03
	C_6H_{14}	0.07
	$C_{10}H_{22}$	0.2
	$C_{15}H_{32}$	0.15
	$C_{20}H_{42}$	0.05
Water viscosity (cp)		0.337
Water Compressibility (1/psi)		$3.0x10^{-5}$
Rock Compressibility (1/psi)		1.0e-6
Simulation Time (day)		730.0
Constant Time Step Size (day)		0.1
Injector Well Top Location (I,J,K)		(1,1,1)
Injector Well Bottom Location (I,J,K)		(1,1,5)
Injection Bottomhole Pressure (psi)		1700
Injection Fluid Composition	CH_4	0.77
	C_3H_8	0.20
	C_6H_{14}	0.03
Producer Well Top Location (I,J,K)		(10,10,1)
Producer Well Bottom Location (I,J,K)		(10,10,5)
Production Bottomhole Pressure (psi)		1300

Table 3.10 (Cont.)

Relative Permeability functions used for generating the tables:

$$K_{r1} = 0.4089\left(\frac{S_1 - 0.2}{0.5}\right)^3$$

$$K_{r21} = \left(\frac{0.7 - S_1}{0.5}\right)^2$$

$$K_{r3} = 0.39\left(\frac{S_3 - 0.05}{0.6}\right)^3$$

$$K_{r23} = 0.83886\left(\frac{0.65 - S_3}{0.6}\right)^{2.1952}$$

Capillary Pressure functions used for generating the tables:

$$P_{c21} = 0.05 + 255.5328\exp(-8.689S_1)$$

$$P_{c23} = 6.00524x10^{-4}\exp(13.544618S_3)$$

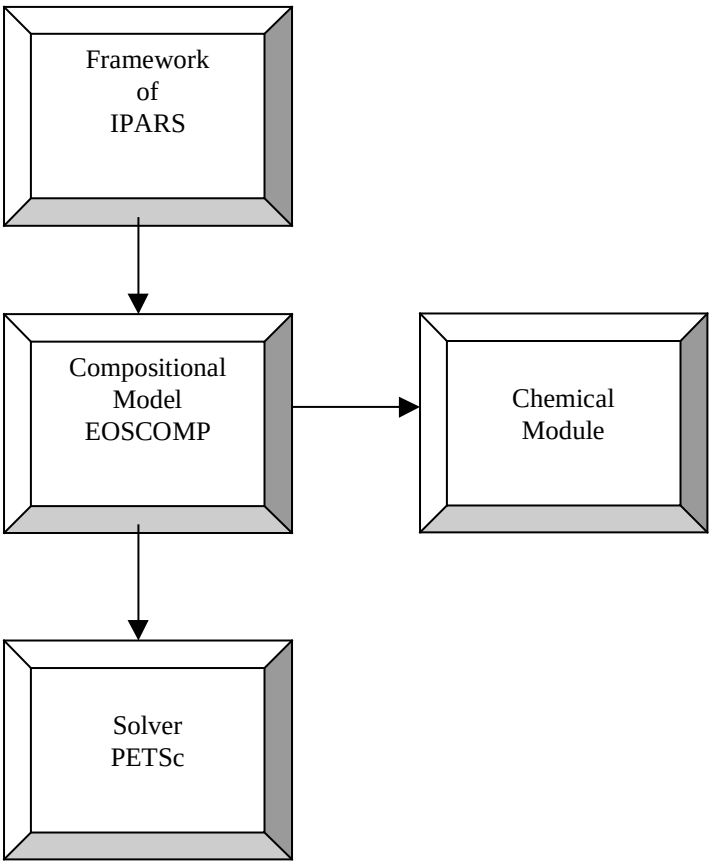

Figure 1.1: Flow chart showing the general structure of GPAS simulator

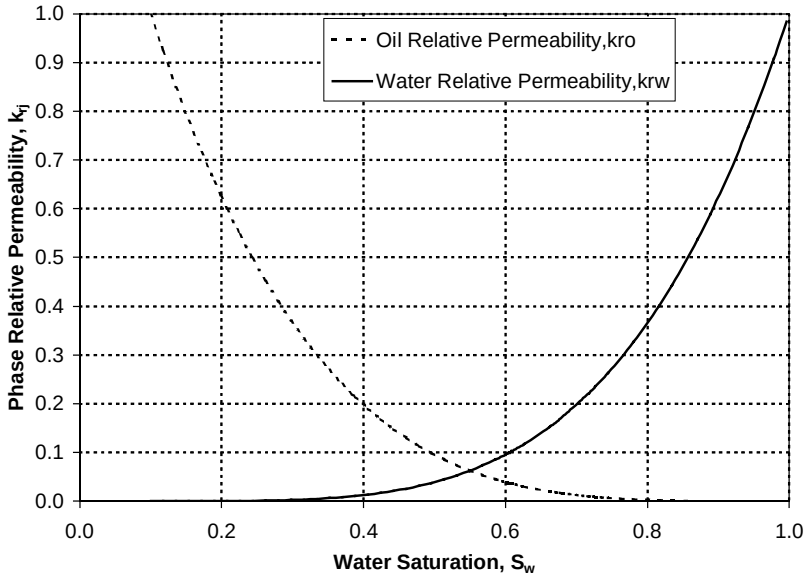

Figure 3.1: Oil/Water relative permeability curves used in the Buckley Leverett Problem.

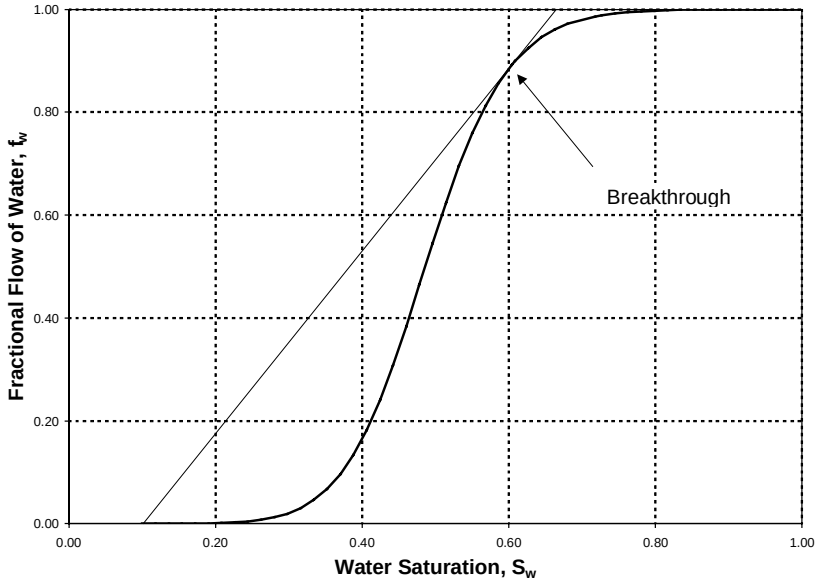

Figure 3.2: Fractional flow curve of water in the Buckley Leverett Problem.

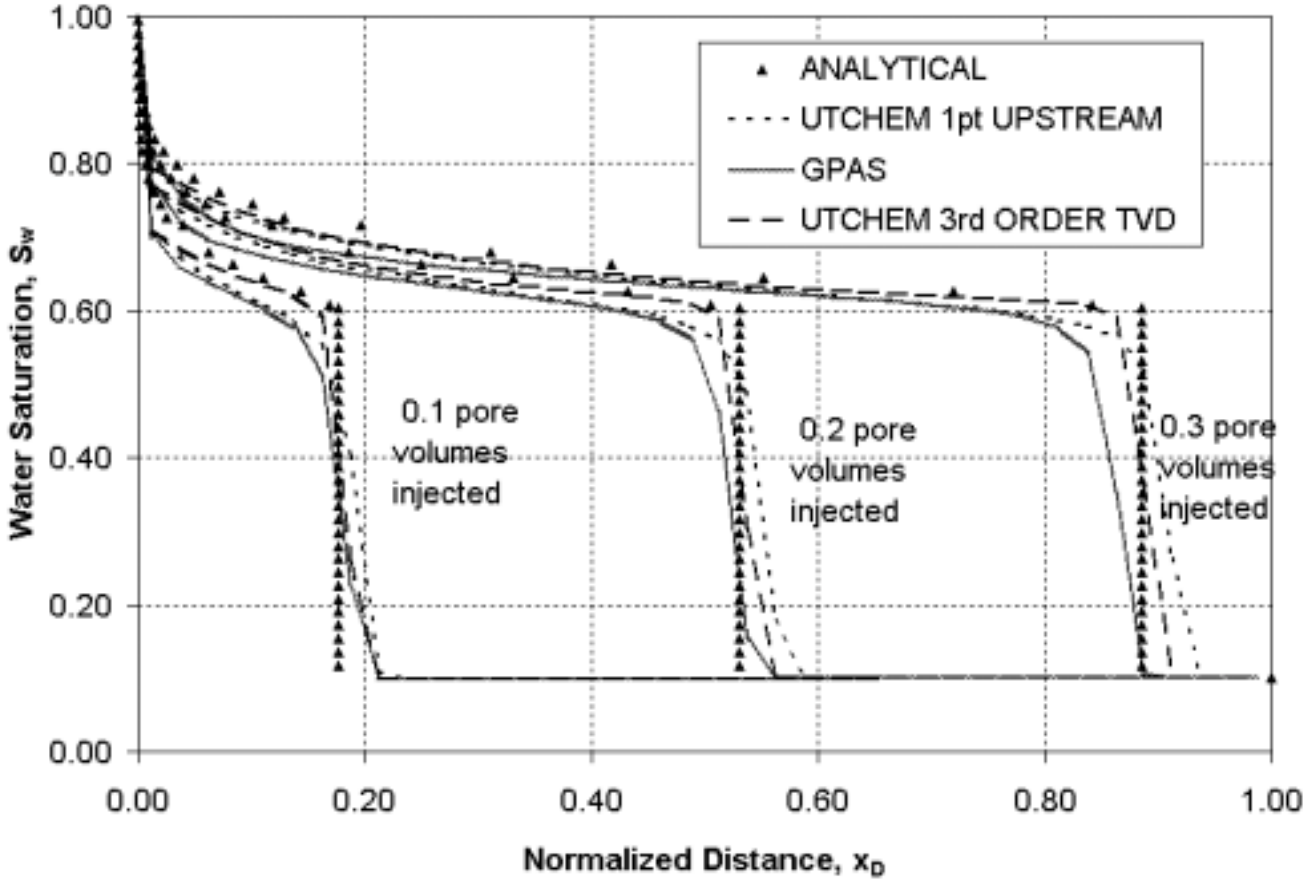

Figure 3.3: Comparison of the water saturation profile from GPAS with the analytical solution and the result from UTCHEM at 0.1, 0.2 and 0.3 pore volumes injected for one-dimensional Buckley Leverett waterflooding

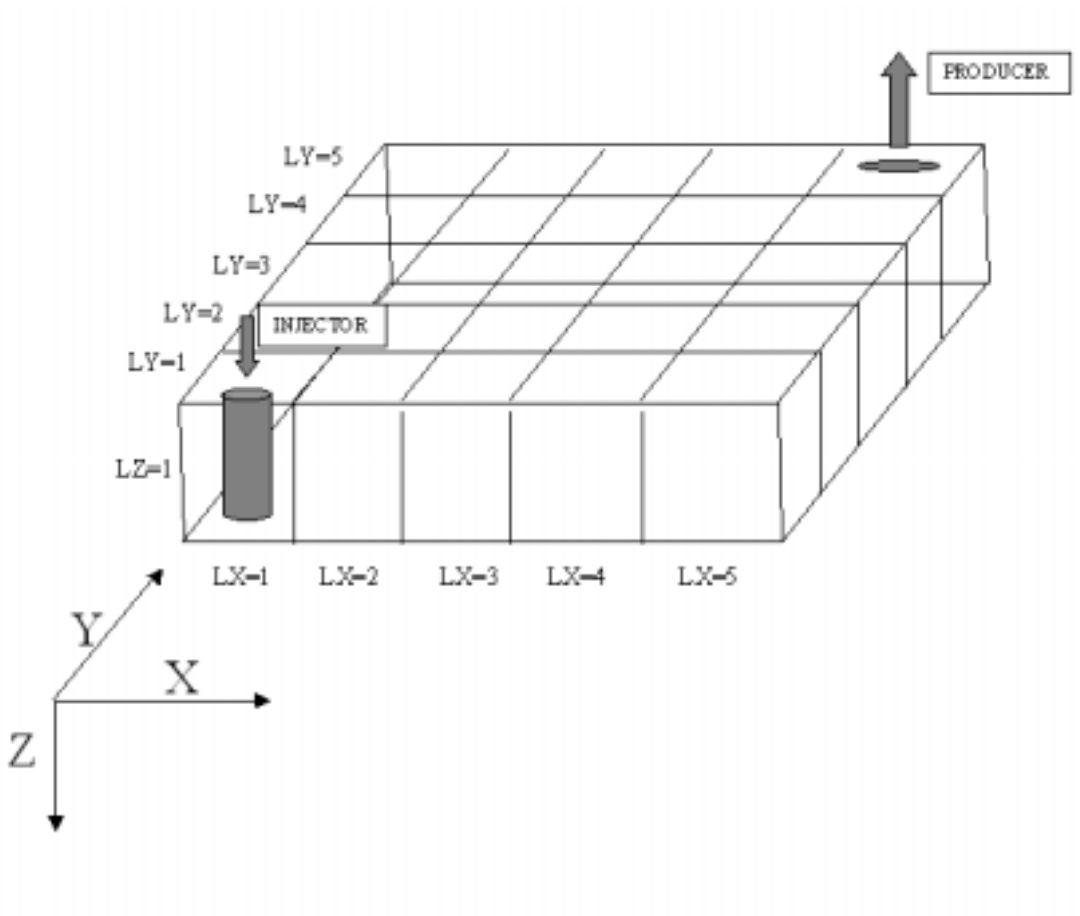

Figure 3.4: Schematic reservoir geometry (quarter five spot) for the CO_2 sequestration problem.

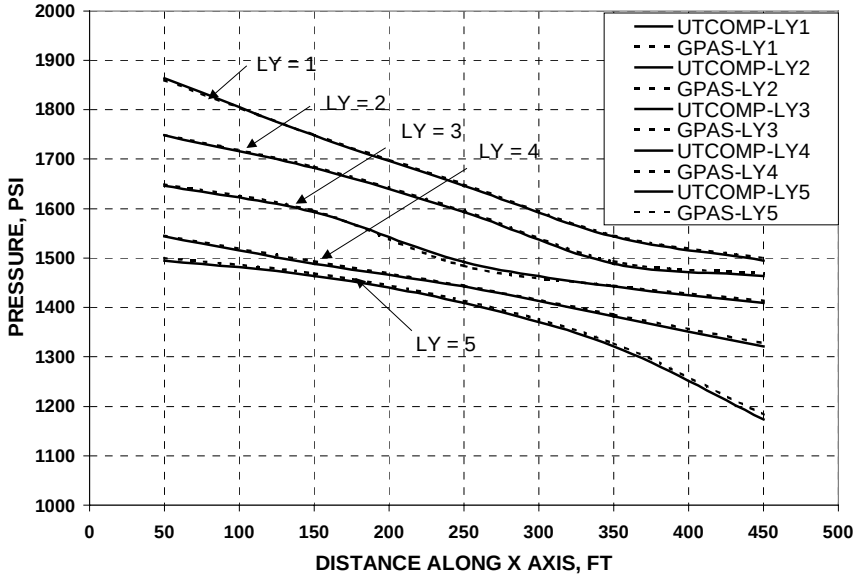

Figure 3.5: Comparison of the pressure profile along the x-axis obtained from GPAS with UTCOMP at the end of 100 days for CO_2 sequestration problem.

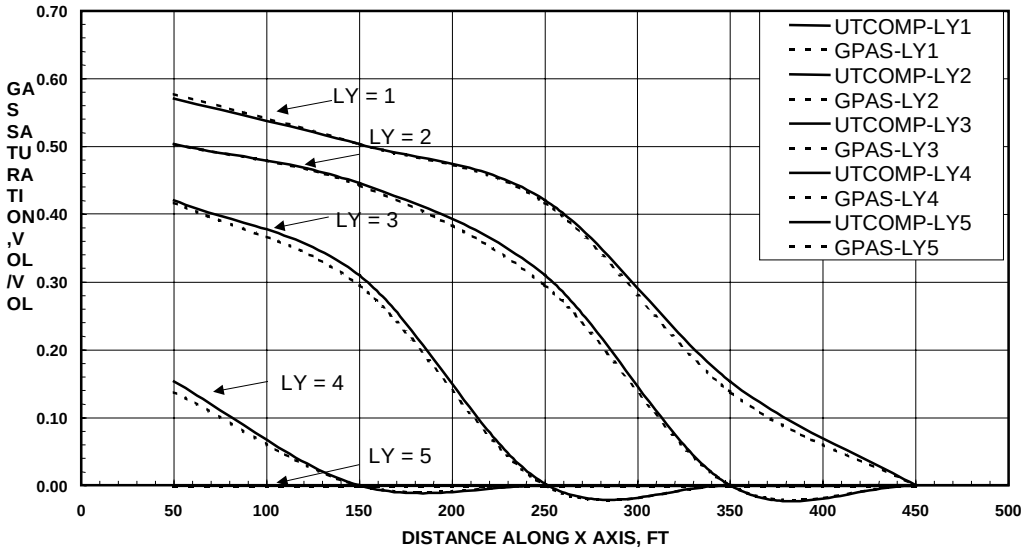

Figure 3.6: Comparison of the gas saturation profile along the x-axis from GPAS with UTCOMP at the end of 100 days for the CO_2 sequestration problem.

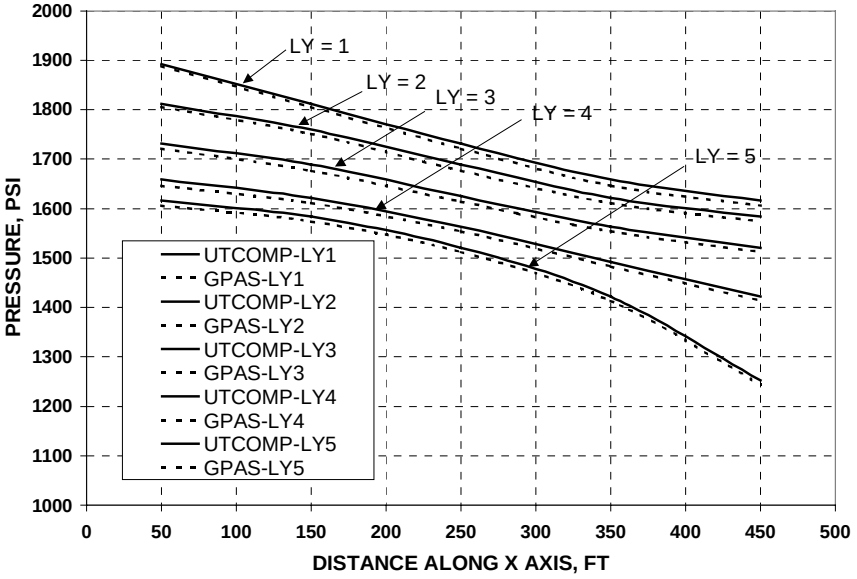

Figure 3.7: Comparison of the pressure profile along the x-axis from GPAS with UTCOMP at the end of 100 days for the six component problem.

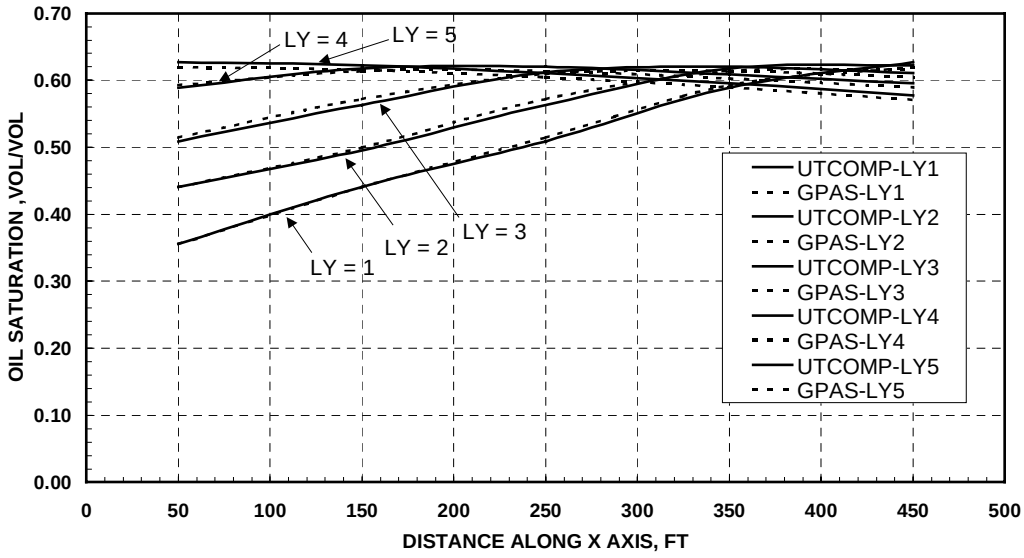

Figure 3.8: Comparison of the oil saturation profile along the x-axis from GPAS with UTCOMP at the end of 100 days for the six component problem.

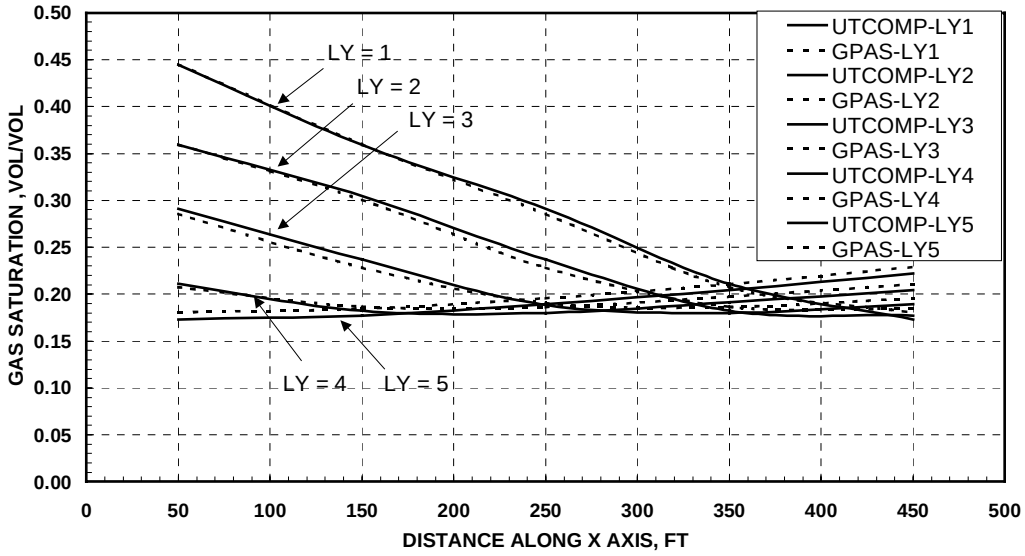

Figure 3.9: Comparison of the gas saturation profile along the x axis from GPAS with UTCOMP at the end of 100 days for the six component problem.

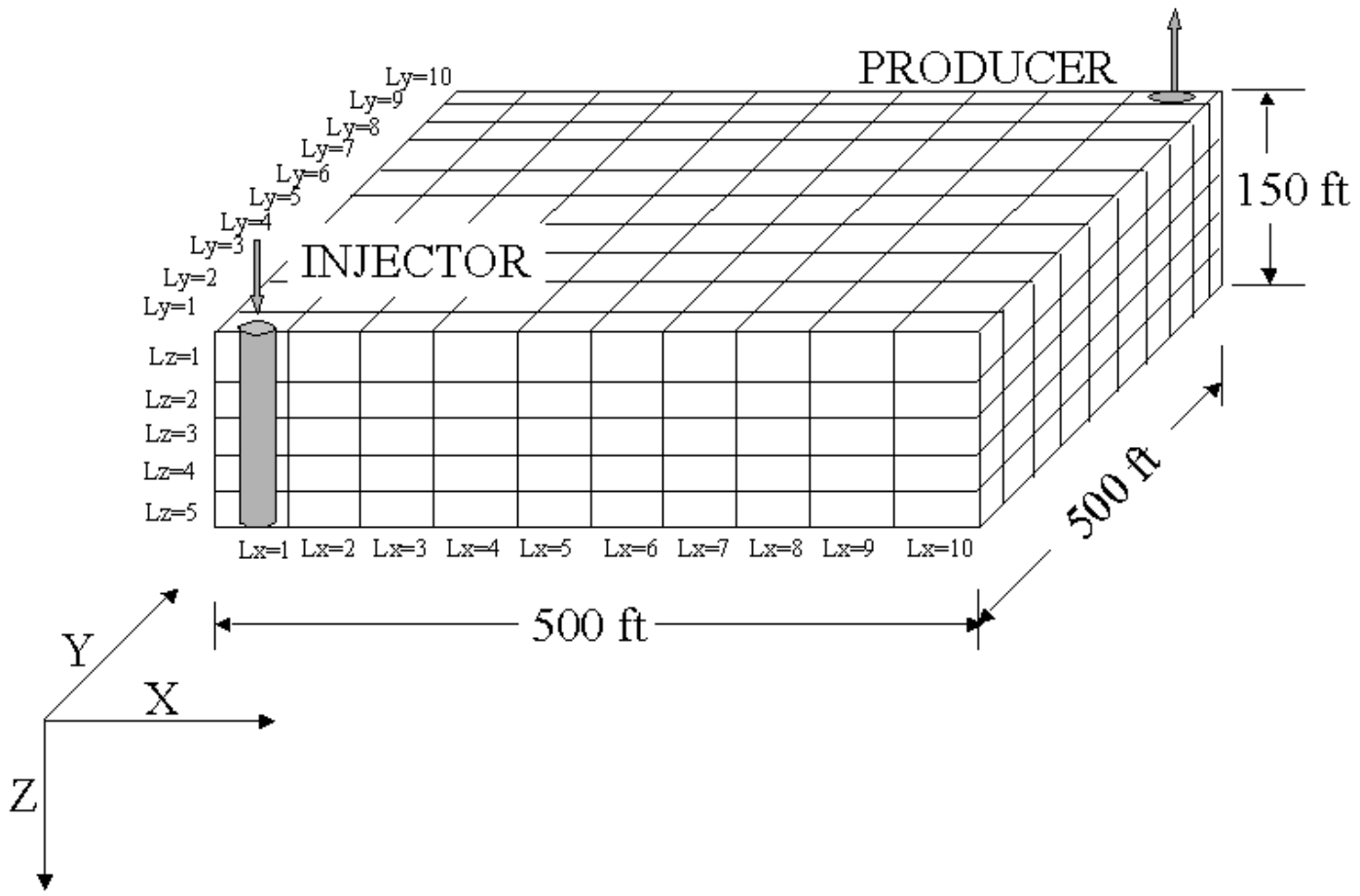

Figure 3.10 Schematic reservoir geometry for the three dimensional six component simulation case.

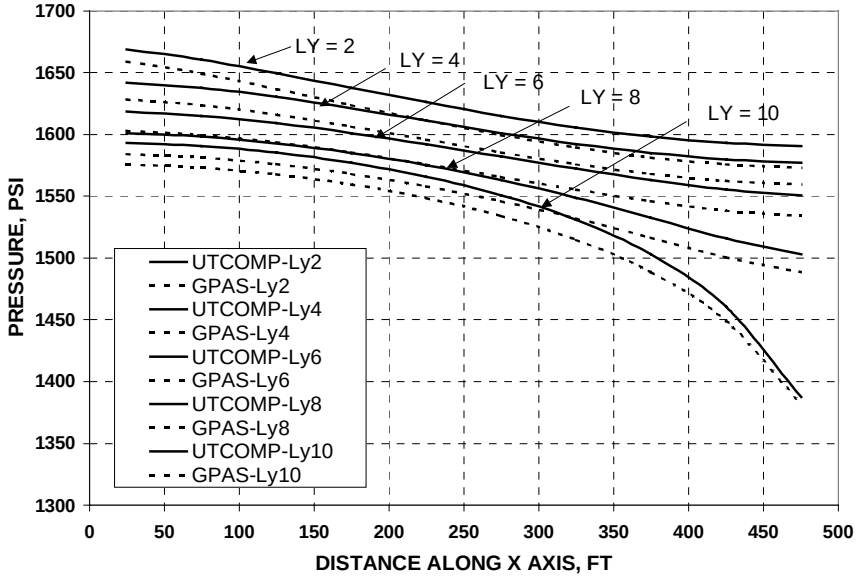

Figure 3.11: Comparison of the pressure profile along the x-axis from GPAS with UTCOMP for the six component case at the end of two years.

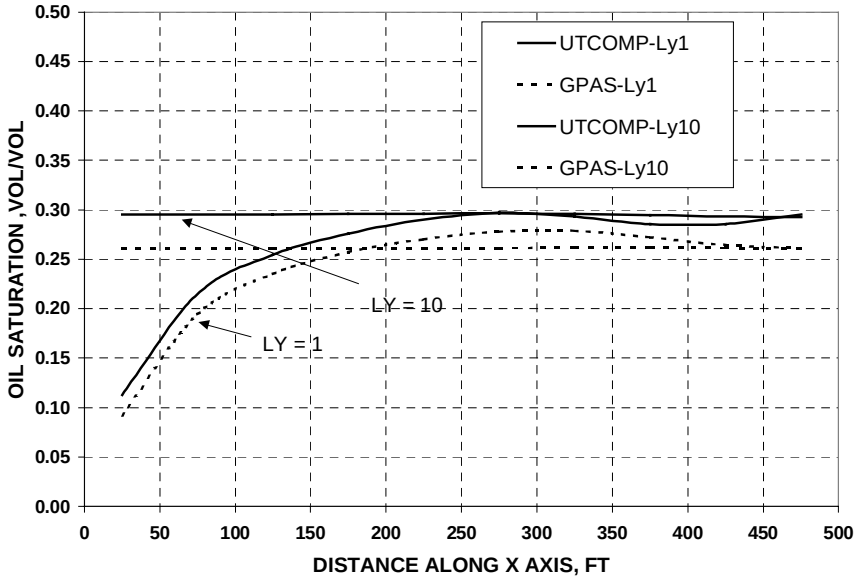

Figure 3.12: Comparison of the oil saturation profile along the x-axis from GPAS with UTCOMP for the six component case at the end of two years.

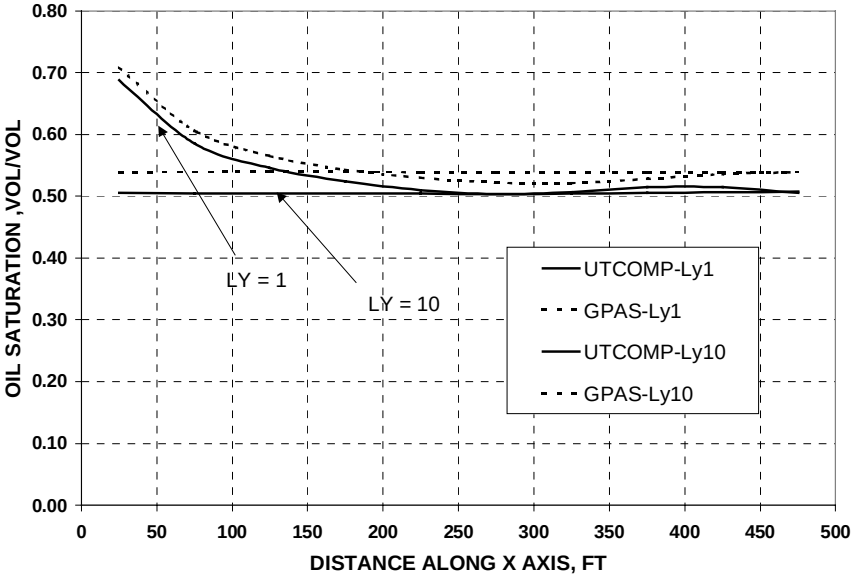

Figure 3.13: Comparison of the gas saturation profile along the x-axis from GPAS with UTCOMP for the six component case at the end of two years.

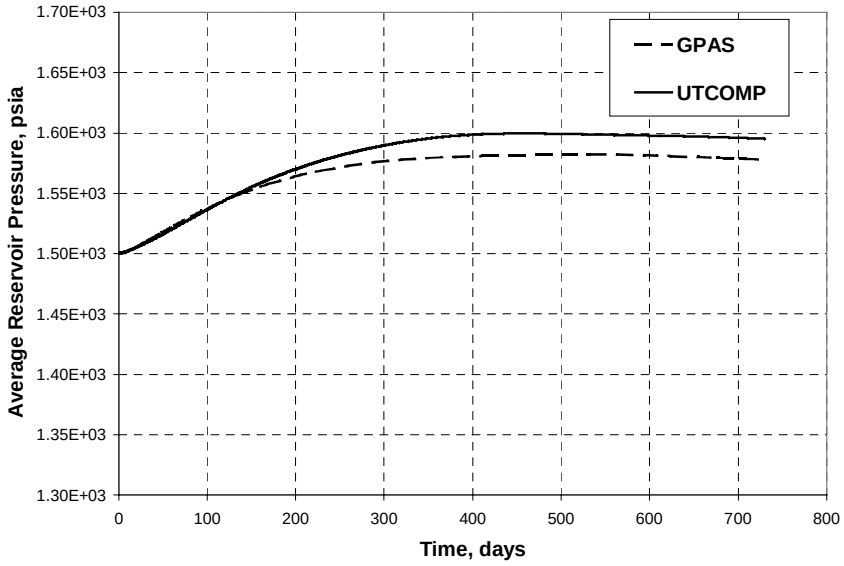

Figure 3.14: Comparison of the average reservoir pressure history from GPAS with UTCOMP for the six component case.

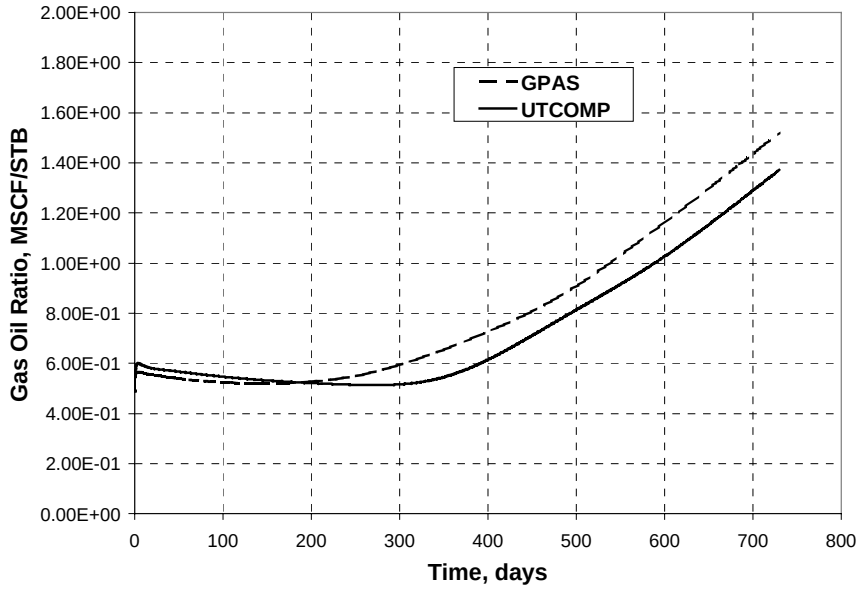

Figure 3.15: Comparison of the producer GOR (gas-oil ratio) history of GPAS with UTCOMP result for the six component case.

REFERENCES

Aziz, K., Ramesh, B., and Woo, P.T.:" Fourth SPE Comparative Solution Project: A Comparison of Steam Injection Simulators", SPE 13510 presented at the Eighth SPE symposium on Reservoir Simulation, Dallas, TX, 1985.

Baker, L.E., Pierce, A.C. and Luks, K.D.:" Gibbs Energy Analysis of Phase Equilibria," Society of Petroleum Engineers Journal, 22, No.5, 1982.

Balay, S., Gropp, W., McInnes, L.C. and Smith, B.:" Efficient Management of Parallelism in Object Oriented Numerical Software Libraries," Modern Software Tools in Scientific Computing, Argonne National Laboratory, October 1997.

Chang, Y.B.: Development and Application of an Equation of State Compositional Simulator, Ph.D. Dissertation, 1990.

Delshad, M., Pope, G.A., and Sepehrnoori, K.:" A Compositional Simulator for Modeling Surfactant Enhanced Aquifer Remediation," Journal of Contaminant Hydrology, 23, 1996.

Delshad, M.: Trapping of Micellar Fluids in Berea Sandstone, Ph.D. Dissertation, The University of Texas at Austin, 1990.

Gosset, H. and Kalitventzeff.:" An Efficient Algorithm to Solve Cubic Equations of State," Fluid Phase Equilibria, 25 ,1986.

Gropp, W., Morgan, T., Smith, B., Arbogast, T., Dawson, C.N., Lake, L.L., McKinney, D.C., Pope, G.A., Sepehrnoori, K., and Wheeler, M.F.: *New Generation Framework For Petroleum Reservoir Simulation*,First Annul Report, May 31, 1996, Advanced Computational Technology Initiative, Argonne National Laboratory and The University of Texas at Austin.

Killough, J.E. and Kossack, C.A.:" Fifth Comparative Solution Project: Evaluation of Miscible Flood Simulators," SPE 16000, presented at the ninth SPE symposium on Reservoir Simulation held in San Antonio, Texas, February, 1987.

Leibovici, C.F. and Neoschil, J.:" A New Look at the Rachford-Rice Equation for Flash Calculations," Fluid Phase Equilibria, 1992.

Liu J., Pope, G.A., and Sepehrnoori, K.:" A High Resolution, Fully Implicit Method for Enhanced Oil Recovery Simulation," SPE 29098 presented at the 13th SPE Symposium on Reservoir Simulation held in San Antonio, TX, February 12-15, 1995.

Lohrenz, J., Bray, B.G. and Clark, C.R.: "Calculating Viscosities of Reservoir Fluids from their Compositions," Trans., AIME, 1964.

Maroongroge, V.: Modeling and application of tracers for reservoir characterization, Ph.D. Dissertation, The University of Texas at Austin, 1994.

Michelsen, J.L.:" The Isothermal Flash Problem. Part I. Stability," Fluid Phase Equilibrium, 1982.

Parashar M., Wheeler, J.A., Pope G.A., Wang, K., and Wang, P.:" A New Generation EOS Compositional Reservoir Simulator: Part II - Framework and Multiprocessing," SPE 37977 presented at the 1997 SPE Reservoir Simulation Symposium, June 8-11, USA.

Peng, D.Y. and Robinson, D.B." A New Two-Constant Equation of State," Ind. Eng. Chem. Fundam., 1976.

Perschke, D.R.: Equation of State Phase Behavior Modeling for Compositional Simulator, Ph.D. Dissertation, University of Texas at Austin, 1988.

Reid, R.C., Prausnitz, J.M. and Poling, B.E.: *The Properties of Gases and Liquids*, Fourth Edition, McGraw-Hill, Inc., NY, 1987.

Smith, J.M. and Van Ness, H.C.: *Introduction to Chemical Engineering Thermodynamics*, McGraw-Hill, Inc., NY, 1975.

Sandler, Stanley I.*: Chemical and Engineering Thermodynamics*, Third Edition, John Wiley & Sons, Inc., 1999.

Trangenstein, J.A.," Customized Minimized Techniques for Phase Equilibrium Computations in Reservoir Simulation," Chem. Eng. Sci., 42, No.12, 1987.

Wang, P., Balay, S., Sepehrnoori, K., Wheeler, J., Abate, J., Smith, B. and Pope,

G.A.:" A Fully Implicit Parallel EOS.Compositional Simulator for Large Scale Reservoir Simulation," SPE 51885 presented at the 1999 SPE 15th Reservoir Simulation Symposium, Houston, TX, Feb. 14-17, 1999.

Wang, P., Yotov, I., Wheeler, M., Arbogast, T., Dawson, C., Parashar, M. and Sepehrnoori, K.:" A New Generation EOS Compositional Reservoir Simulator: Part I - Formulation and Discretization," SPE 37979 presented at the 1997 SPE Reservoir Simulation Symposium, USA.

Wheeler, J., *et al.: IPARS user's manual*, October 8,2000, University of Texas at Austin.